

pubs.acs.org/est Article

Application of High-Resolution Mass Spectrometry to Evaluate UV-Sulfite-Induced Transformations of Per- and Polyfluoroalkyl Substances (PFASs) in Aqueous Film-Forming Foam (AFFF)

Raul Tenorio, Andrew C. Maizel, Charles E. Schaefer, Christopher P. Higgins, and Timothy J. Strathmann*



Cite This: Environ. Sci. Technol. 2022, 56, 14774–14787



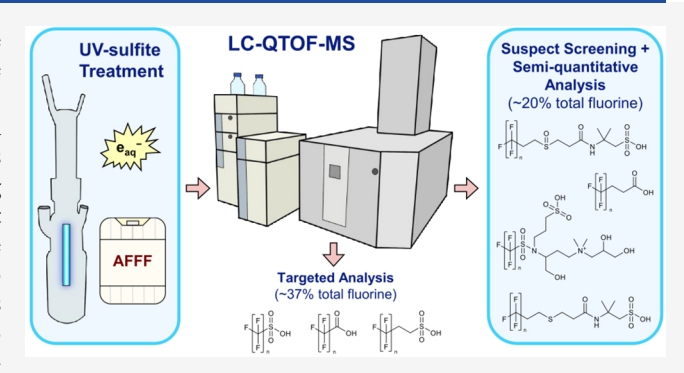
ACCESS I

III Metrics & More

Article Recommendations

Supporting Information

ABSTRACT: UV-sulfite has been shown to effectively degrade per- and polyfluoroalkyl substances (PFASs) in single-solute experiments. We recently reported treatment of 15 PFASs, including perfluoroalkyl sulfonic acids (PFSAs), perfluoroalkyl carboxylic acids (PFCAs), and fluorotelomer sulfonic acids (FTSs), detected in aqueous film-forming foam (AFFF) using high-resolution liquid chromatography quadrupole time-of-flight mass spectrometry (LC-QTOF-MS) targeted analysis. Here, we extend the analysis within those original reaction solutions to include the wider set of PFASs in AFFF for which reactivity is largely unknown by applying recently established LC-QTOF-MS suspect screening and semiquantitative analysis protocols. Sixtyeight additional PFASs were detected (15 targeted + 68 suspect



screening = 83 PFASs) with semiquantitative analysis, and their behavior was binned on the basis of (1) detection in untreated AFFF, (2) PFAS photogeneration, and (3) reactivity. These 68 structures account for an additional 20% of the total fluorine content in the AFFF (targeted + suspect screening = 57% of total fluorine content). Structure–reactivity trends were also revealed. During treatment, transformations of highly reactive structures containing sulfonamide $(-SO_2N-)$ and reduced sulfur groups (e.g., -S- and -SO-) adjacent to the perfluoroalkyl $[F(CF_2)_n-]$ or fluorotelomer $[F(CF_2)_n(CH_2)_2-]$ chain are likely sources of PFCA, PFSA, and FTS generation previously reported during the early stages of reactions. The results also show the character of headgroup moieties adjacent to the $F(CF_2)_n-F(CF_2)_n(CH_2)_2-$ chain (e.g., sulfur oxidation state, sulfonamide type, and carboxylic acids) and substitution along the $F(CF_2)_n-$ chain (e.g., H-, ketone, and ether) together may determine chain length-dependent reactivity trends. The results highlight the importance of monitoring PFASs outside conventional targeted analytical methodologies.

KEYWORDS: suspect screening, advanced reduction processes (ARPs), precursors, structure-reactivity trends

INTRODUCTION

The use of aqueous film-forming foam (AFFF) in fire training activities conducted at military, commercial, and municipal facilities has been implicated as a major source of contamination of drinking water sources by per- and polyfluoroalkyl substances (PFASs). Increased PFAS levels, up to concentrations on the order of $10-100~\mu g~L^{-1}$, have been detected in ground and surface waters near fire training areas where AFFF was used. ²⁻⁴ Select routinely measured PFASs have also been detected at nanogram per liter levels in groundwaters at AFFF-impacted sites. ⁵ Consumption of PFAS-contaminated water, linked to adverse health effects, including effects on the immune system and the cardiovascular system, human development, and cancer, ⁶ has impacted millions of people in the United States. ⁴ AFFFs are mixtures of fluorocarbon and hydrocarbon surfactants with co-solvents and corrosion inhibitors that can be applied to rapidly

extinguish fuel-based fires.⁷ The fluorocarbon surfactant portion of individual AFFF formulations contains a proprietary mixture of PFASs, typically dominated by either perfluoroalkyl sulfonic acid (PFSA) or fluorotelomer acid derivatives.^{1,8,9} Thus, AFFF-impacted water sources are contaminated by a mixture of PFASs that is highly dependent upon the AFFF source material, the distance from the source, and the time since environmental release.^{4,10} The presence of these complex PFAS mixtures adds a significant challenge to treatment system design and monitoring.

Received: May 6, 2022 Revised: August 26, 2022 Accepted: August 29, 2022 Published: September 26, 2022





An increasing number of studies have reported on UV-sulfite treatment of PFASs. 11-19 Sulfite (SO₃²⁻) is a photosensitizer that ejects highly reductive hydrated electrons (e_{aq}^{-} ; $E_{H}^{0} = -2.9 \text{ V}$)²⁰ when irradiated with UVC light sources.²¹ Sulfite photolysis also generates sulfite radicals (SO₃•-). However, SO₃ • are not known to participate in PFAS transformation reactions. Instead, further reactions of SO₃ •- lead to formation of a mixtures of sulfate (SO_4^{2-}) and dithionate $(S_2O_6^{2-})^{18}$ Previous reports have documented the success of UV-sulfite and other processes that generate e_{aq}^{-} (e.g., UV-iodide)²² in degrading PFASs that are normally recalcitrant to other destructive treatment technologies, including perfluorooctanesulfonate (PFOS). 11,12 Though AFFF-impacted groundwaters contain complex PFAS mixtures, most studies have focused on experiments treating individual PFASs, most often perfluoroalkyl acids (PFAAs) like PFOS and perfluorooctanoic acid (PFOA) in single-solute experiments. 11-13 Only recently have studies been expanded to include a broader range of PFASs beyond PFAAs, 15,23,24 but the range of structures examined still does not represent the full diversity of PFASs identified in

Recently, high-resolution mass spectrometry (HRMS) suspect screening methods, including protocols developed using liquid chromatography with quadrupole time-of-flight mass spectrometry (LC-QTOF-MS), have been applied to characterize the wider suite of PFASs present in AFFF and AFFF-impacted water sources^{1,25,26} and to evaluate sorptive, membrane, and electrochemical treatment of suspect PFASs identified in the mixtures.^{27–29} To the best of our knowledge, HRMS suspect screening analysis has not previously been applied in the study of UV-sulfite treatment of AFFF-containing water sources.

We recently reported on UV-sulfite treatment of PFASs detected in an AFFF mixture by targeted quantitative analysis (i.e., analysis with authentic reference standards), which included a range of PFAAs and fluorotelomer sulfonic acids (FTSs).¹⁴ The results of that work demonstrated that PFAS reactivity was greatly influenced by chemical structure. Longchain PFSAs, long-chain FTSs, perfluoroalkyl carboxylic acids (PFCAs) of all chain lengths, and branched PFSA and PFCA isomers were the most reactive structures, and reaction rate constants observed for individual PFASs in the AFFF were similar to those measured in single-solute experiments. Structure-reactivity trends observed in other work 15,22 were also maintained in AFFF; PFSA and FTS reactivity was dependent on chain length, while PFCA reactivity was independent of chain length for PFCAs (n = 3-7). Curiously, the concentration of some target analytes increased during the initial stages of the reaction, suggesting the presence of additional PFASs in the AFFF that can act as PFAA and FTS precursors during treatment. This conclusion was supported by results showing detected PFASs accounted for only 37% of the total fluorine content of the AFFF and the results from the total oxidizable precursor (TOP) assay that documented, indirectly, the presence of PFAA precursors that could account for an additional 50% of the fluorine in the AFFF. While helpful, the TOP assay does not provide detailed structural information about individual PFAA precursors present or reactivity patterns among different precursor structures. Another study found that targeted analysis also accounted for <50% of the total fluorine in two AFFF formulations (44% and 1%) using similar analytical methods.³⁰

In this work, recently established LC-QTOF-MS suspect screening and semiquantitative analysis protocols³¹ were applied to the original reaction solutions in ref 14 to further characterize UV-sulfite treatment of AFFF. Suspect screening identification of PFASs in the AFFF was accomplished by comparing HRMS data with mass spectra and extracted ion chromatogram (XIC) data for >1400 PFAS analytes that have been initially reported in other work ranging from biotransformation studies to discovery analyses. 25,26,31 Recently introduced semiquantitative analysis protocols, 31 which provide estimates of suspect analyte concentrations based upon ionization patterns of analytical standards with related structures, were then applied to track changes in the estimated concentrations of individual suspect PFASs during UV-sulfite reactions. The findings provide previously undetermined PFAS structure-reactivity insights that can be used to inform process design. The results were then combined with previously reported targeted analysis results of PFAAs and FTSs to identify structure-reactivity patterns and evaluate potential impacts of suspect compound transformations on the net treatment of PFASs that would not be observed using more conventional targeted analytical methodologies (e.g., U.S. EPA Method 537).3

MATERIALS AND METHODS

Chemicals. Chemicals used in reactions, including the AFFF concentrate mixture (donated by Jacobs Engineering), were described previously. PFAS characterization indicates it is a mixture of source materials, including both 3M-based (i.e., electrochemical fluorination process) and fluorotelomer-based AFFFs. A complete list of reagents is provided in the Supporting Information. A list of PFAS native and labeled analytical standards used in LC-QTOF-MS analysis was described previously. 14

Photolysis Experiments. Photochemical reaction equipment and experimental conditions were described in detail previously. 14 Briefly, reactions were performed in an immersion well photoreactor (575 mL) with a jacketed quartz well containing an 18 W low-pressure (LP) Hg lamp. Tests showed a photon flux of $(2.2 \pm 0.5) \times 10^{-6}$ E s⁻¹, an effective path length of 2.85 \pm 0.03 cm, and an average photon fluence rate of 1.0 \times 10⁻⁸ \pm 3.3 \times 10⁻¹¹ E s⁻¹ cm⁻². ¹⁴ Solutions and the light source were temperature-controlled at 20 °C. Sodium sulfite (10 mM) and sodium bicarbonate (5 mM; pH 9.5 buffer) were added to solutions that were vigorously sparged with $N_{2(g)}$ (99%) to remove dissolved oxygen (DO; e_{aq}^{-} scavenger). Sodium bicarbonate was used to buffer the pH to alkaline conditions under which UV-sulfite is most effective due to minimization of H+, which is a eaq scavenger.²⁰ Furthermore, bicarbonate was used due to its relevance in real treatment scenarios in which bicarbonate would be the most abundant natural pH buffer. Sulfite at 10 mM was selected because higher sulfite concentrations (20 mM) showed comparable defluorination.¹⁴ AFFF diluted 1 to 60 000 was spiked into the solution before UV reactions were initiated. The AFFF was added after sparging to avoid potential foaming during reactions, and anoxic solution conditions were maintained by providing a flowing $N_{2(g)}$ blanket in the reactor headspace throughout the course of the reaction. Samples were then collected periodically and stored at 4 °C prior to analysis. All reactions were performed for a duration of 49 h to provide sufficient reaction time to measure $k_{\rm obs}$ values for more slowly reacting PFASs.¹⁴ Reactions were performed in duplicate, and

Table 1. PFASs in AFFF Detected by Target and Suspect Screening Analysis by LC-QTOF-MS

Super Class	Class Acronym	Compound Acronym	Chain Length (n)	Structure	Conce	entratior	ι (μg/L)	Bin		<i>k</i> obs (h ⁻¹))
PFAAs	PFSA ^a	PFNS	9		0.246	±	0.121	P-O-D		2^b	
		PFOS	8	r=1 fi	69.453	±	13.926	P-O-D	0.080	±	0.005
		PFHpS PFHxS	7 6	F	1.197 12.357	±	0.278 1.200	P-O-D P-I-D	0.043 0.018°	±	0.000 0.001
		PFPeS	5	ITI 8 OH	3.549	±	0.497	P-I-D	0.018°	±	0.001
		PFBS	4	LFJ,	1.484	±	0.443	P-I-R	0.010	ÑA	0.002
		PFPrS	3		0.494	±	0.216	P-I-R		NA	
	PFCA ^a	PFOA	7	5.3.0	0.728	±	0.097	P-O-D	0.427	±	0.114
		PFHpA	6	티티	0.296	±	0.026	P-I-D	0.440°	±	0.001
		PFHxA PFPeA	5	. Д. он	1.784	±	0.984	P-O-D	0.462	±	0.003
		PFBA	4 3	[F],	0.374 0.457	±	0.147 0.268	P-I-D P-O-D	0.432° 0.306	±	0.001 0.042
FTSs and FTCAs	X:2 FTS ^a	8:2 FTS	8	0	0.146	±	0.200	P-I-D	0.063¢	±	0.005
1 100 and 1 10/10	X.2110	6:2 FTS	6	F	0.424	±	0.196	P-I-D	0.003 0.012 ^c	±	0.003
		4:2 FTS	4	[] 8 5"	0.029	±	0.012	P-I-R	0.012	ΝA	0.001
		4.2 F13	4	F 3	0.029	I	0.012	F-I-K		IVA	
	V:0 FT04	4.0 FTO 4	4			NIA		U-I-R		NIA	
	X:2 FTCA	4:2 FTCA	4	F OH		NA		U-I-R		NA	
				E-3 A							
	X:3 FTCA	8:3 FTCA	8	[[]_ Å		NA		U-O-D	0.039	±	0.003
		6:3 FTCA	6	. ₩		NA		U-O-R		NA	
		0.3 FTCA	0	FrJ.		INA		0-0-R		IVA	
FTS and FTCA Derivatives				[F] N							
Denvatives	X:2 FTSA	6:2 FTSA ▲ ^g (EtHxSA isomer)	6	NH ₂	0.011	±	0.002	P-I-R		NA	
				[F]							
	X:2 FTSO2PrAd-DiMeEtS	6:2 FTSO2PrAd-DiMeEtS	6	F N N N N N N N N N N N N N N N N N N N	0.108	±	0.031	P-O-R		NA	
				[F], II H O							
	X:2 FTSO-PrAd-DiMePrS	8:2 FTSO-PrAd-DiMePrS	8	[F] 0 , 0	14.820	±	1.459	P-O-D		NA	
		6:2 FTSO-PrAd-DiMePrS	6	· · · · · · · · · · · · · · · · · · ·	27.138	±	0.136	P-O-D	1.56	±	0.142
		4:2 FTSO-PrAd-DiMePrS	4	L[t]	0.714	±	0.028	P-O-D	4.17 ^d	±	0.53
				[F] o							
	X:2 FTThPrA	6:2 FTThPrA	6		0.556	±	0.002	P-I-D	1.200c,d	±	0.033
	X.2 1 1111 1X	0.211111117	Ŭ	F F S OH	0.000	-	0.002	1.10	1.200	-	0.000
	X:2 FTTh-PrAd-DiMeEtS	8:2 FTTh-PrAd-DiMeEtS	8		1 050		1.513	P-O-D		2e	
	X.2 FTTTI-PTAG-DIMEELS			f	1.859	±			0.004		0.40
		6:2 FTTh-PrAd-DiMeEtS	6	F S N N N N N	13.017	±	6.366	P-O-D	3.28 ^d	±	0.19
		4:2 FTTh-PrAd-DiMeEtS	4	5.3	1.224	±	0.091	P-O-D	4.25 ^d	±	0.14
Fluorotelomer				f o i							
sulfonates/sulfates	X:2 FTSO2PrA	6:2 FTSO2PrA	6	F S OH	0.524	±	0.033	P-O-D	0.028	±	0.006
				r.l." "							
PFSA Derivatives	PFSAi	PFOSi	8	[F] Î		NA		U-I-D	0.083^{c}	±	0.005
		PFPeSi	5	F++S OH		NA		U-I-R		NA	
		PFPrSi	3	[Ė],		NA		U-I-R		NA	
Substituted PFAA	H-PFCA ^h	H-PFOA	6	run M		NA		U-I-D	0.043^{c}	±	0.003
Derivatives		H-PFHpA	5	FUNDH		NA		U-I-D	0.054^{c}	±	0.006
		H-PFHxA	4	III + II	0.039	±	0.000	P-I-D	0.045c	±	0.001
		H-PFPeA	3	F.J. O		NA		U-I-D	0.037 ^{c,d}	±	0.008
	H-PFSA ^h	H-PFOS	7	[=] H o	0.328	±	0.011	P-I-D	0.055	±	0.002
		H-PFPeS	4	F O OH	0.001	±	0.000	P-I-R		NA	
		H-PFBS	3	F i	0.002	±	0.000	P-I-R		NA	
		H-PFPrS	2	2 3 1	0.016	±	0.000	P-I-R		NA	
	K-PFSA	K-PFOS	6	_ [F]	0.164	±	0.015	P-O-D	1.75 ^d	±	0.10
		K BED. O	•	E J J JOH	0.000		0.000	B 0 B	0.5744		0.070
		K-PFPeS	3	F [F],	0.003	±	0.000	P-O-D	0.571 ^d	±	0.070
	O-PFSA	O-PFHpS	5	- [F] P	0.031	±	0.000	P-O-R		NA	
			_	, OH BOH							
		O-PFPeS	3	F [F],	0.001	±	0.000	P-I-R		NA	
	X:1 PFSA ^h	7:1 PFOS	7	[F] Q	0.124	±	0.012	P-I-D	0.011c	±	0.002
				F → Ši OH							
		6:1 PFHpS	6	[F] O		NA		U-I-R		NA	
Cyclic and	H-UPFSA ^h	H-UPFOS	4	F [[F] [0.034	±	0.003	P-I-D	0.047°	±	0.002
Unsaturated PFAAs		H-UPFHxS	2	F		NA		U-I-R		NA	
		H-UPFPeS	1	F F [F]		NA		U-I-R		NA	
	UPFSA ^h	UPFOS ■g	5	f	0.830	±	0.053	P-O-D		2 ^b	
	0.1.071			F OH	0.000		0.000			_	
		UPFPeS	2	,		NA		U-I-D	0.041°	±	0.001
				[F] F F OH							
	CHxS	PFEtCHxS ■g (UPFOS isomer)	8 (x = 2)	F.OH	0.830	±	0.053	P-O-D		2 ^b	
	CHAS	FI Etorixo • (OFT OS Isomer)	0 (x - 2)	F[F] \ S o	0.000	_	0.000	1-0-0		~	
0.46	A D . E4.04	A - D - EU - O A		FF FFO	0.404		0.000		0.400		0.004
Sulfonamide Precursors	AmPr-FASA	AmPr-FHxSA AmPr-FPeSA	6 5	_[F] Î	2.101 0.344	±	0.089 0.003	P-O-D P-O-D	0.103 0.104	±	0.024 0.011
1 100013013		AmPr-FBSA	4	,44g,A~~dt	0.384	±	0.003	P-O-D	0.099	±	0.009
		AmPr-FPrSA	3	[+],	0.188	±	0.003	P-O-D	0.099	±	0.003
	AmPr-FASA-PrA	AmPr-FHxSA-PrA	6	О₩ОН	2.426	±	0.336	P-O-D		ÑΑ	
		AmPr-FPeSA-PrA	5	[-16]	0.495	±	0.038	P-O-D	1.42	±	0.01
		AmPr-FBSA-PrA	4	F. S. N. ~ NH	0.567	±	0.023	P-O-D	0.935	±	0.033
		AmPr-FPrSA-PrA	3	[F] ö " ~ ~ "" (0.301	±	0.023	P-O-D	0.470	±	0.074
	CM-A-D- 5404			r-10							
	CMeAmPr-FASA	CMeAmPr-FHxSA	6	FJF S	0.092	±	0.001	P-O-D	0.156	±	0.031
		CMeAmPr-FBSA	4	[]öĦ /\ [0.011	±	0.000	P-O-D	3.0'	±	0.2
				0×20H		_					-
				F-18							
	CMeAmPr-FASAPrA	CMeAmPr-FHxSAPrA	6	F\$\$\$\frac{1}{2}\display \display \din \display \display \display \display \display \display \display	0.088	±	0.009	P-O-D	1.03 ^d	±	0.09
				[] o ~~ OH							
				Q _n OH							
				750							
	DiMeA-MeOHPr-FASAPrS	DiMeA-MeOHPr-FHxSAPrS	6		0.063	±	0.004	P-O-D		NA	
				1 8 m							
				ОН							
	diOHPrAm-MeOHPr-FASA	diOHPrAm-MeOHPr-FHxSA	6	E-1.9 COH	0.177	±	0.002	P-O-D	0.137	±	0.005
		diOHPrAm-MeOHPr-FPeSA	5	FIFE N	0.034	±	0.003	P-O-D	0.099	±	0.015
		diOHPrAm-MeOHPr-FBSA	4	[] ö H /\ oH	0.037	±	0.001	P-O-D		NA	
	diOHPrAm-MeOHPr-FASAPrS		6	. OH			0.221	P-O-D		3.20 ^d	
	GIODELATIF-MECHET-FASAPIS	diOHPrAm-MeOHPr-FHxSAPrS		0 k = 0	1.099	±					
		diOHPrAm-MeOHPr-FPeSAPrS	5	[F] Y	0.293	±	0.018	P-O-D	3.20^{d}	±	0.18
		diOHPrAm-MeOHPr-FBSAPrS	4	FH BN NOT OH	0.497	±	0.025	P-O-D	2.16^{d}	±	0.11
		diOHPrAm-MeOHPr-FPrSAPrS	3	[[‡]], OH	0.236	±	0.006	P-O-D	0.958^{d}	±	0.044
			-	r.a Q		_				-	
	EtFASA	EtFHxSA ▲g (6:2 FTSA isomer)	6	F	0.011	±	0.002	P-I-R		NA	
	Zii AOA	La Fixon =- (o.2 Fish isoliter)	3	[i] ö A	0.011	±	0.002	1 -1-17		14/	

Table 1. continued

Super Class Class	Acronym Compound Acronym	Chain Length (n)	Structure	Conce	entration	(µg/L)	Bin		<i>k</i> _{obs} (h ⁻¹)	
FASA	FBSA	4	_ [F] Q	0.443	±	0.081	P-O-D		NA	
	FPrSA	3	FJ NH2	0.175	±	0.031	P-O-D		NA	
MeFASA	MeFHxSA	6	F = 0 0 0 0 0 0 0 0 0 0 0 0 0 0 0 0 0 0	0.004	±	0.000	P-O-R		NA	
MeFASAA ●g	MeFPeSAA	5	[-] S	0.208	±	0.005	P-O-D	0.351	±	0.006
	MeFBSAA	4	F N OH	0.328	±	0.005	P-O-D		NA	
	MeFPrSAA	3	[F] 0	0.148	±	0.006	P-O-D		NA	
FASA-PrA ●g (I	MeFASAA FPeSA-PrA	5	[F] P P	0.208	±	0.005	P-O-D	0.351	±	0.006
isomer)	FBSA-PrA	4	F S N OH	0.328	±	0.005	P-O-D		NA	
	FPrSA-PrA	3	[+],	0.148	±	0.006	P-O-D		NA	
OAmPr-FASA	OAmPr-FHxSA	6	F F S N N OH	0.094	±	0.006	P-O-D	0.106	±	0.019
SPrAmPr-FAS	A SPrAmPr-FHxSA	6		0.728	±	0.019	P-O-D	0.095	±	0.003
	SPrAmPr-FPeSA	5	F. [F]	0.117	±	0.000	P-O-D	0.076	±	0.004
	SPrAmPr-FBSA	4	Han A X A	0.121	±	0.000	P-O-D	0.073	±	0.009
	SPrAmPr-FPrSA	3	C-34	0.055	±	0.001	P-O-D	0.073	±	0.006
SPr-FASA	SPr-FHxSA	6	[=] []	0.109	±	0.005	P-O-D		NA	
	SPr-FBSA	4	F S N N S OH		NA		U-O-D		0.117	
	SPr-FPrSA	3	[+], " "	0.007	±	0.000	P-O-D		NA	

"Compounds in the PFSA, PFCA, and X:2 FTS class were reported previously using targeted analysis." La Estimated by the initial rate method using two points. Calculated from the maximum concentration formed. ${}^dk_{\rm obs}$ estimate (only two or three points available). Lower bound estimate (only one point available). Estimated by linear extrapolation. Matching symbols indicate isomeric structures (isomers listed in Table S3). Multiple isomers possible for H-PFCA, H-PFSA, X:1 PFSA, H-UPFSA, and UPFSA.

averages are reported with uncertainties as minimum/ maximum values.

LC-QTOF-MS Analysis. Detailed chromatographic methods were described previously. 14 LC-QTOF-MS analysis was used in electrospray ionization negative (ESI-) mode to conduct suspect screening analysis against an MS/MS library of >300 PFASs and a custom XIC list of >1400 molecular formulas and masses of suspected PFASs derived from recent discovery analyses and inferred homologues.^{27,31,33,34} ESI⁻ mode was selected due its established use in PFAS analysis and availability of standards that can be ionized by ESI mode compared to the limited availability of standards that can be analyzed by ESI+ mode. 7,31,35

Suspect Screening and Semiquantitative Analysis. Data were acquired and processed using SCIEX OS version 1.3 to identify PFASs for which no standards were available by screening against an XIC list and MS/MS library. Only PFASs with peak areas of >20 (peak area range of 233-1767 627; average peak area of 65 531) and eluting at retention times of >5 min were considered; retention times of <5 min likely reflect analytical noise (PFBA eluted at 6.3 min).³⁶ PFASs were then screened using the following criteria: mass error (parts per million), isotope ratio difference, and spectral library match. A custom R script (version 3.6.1) was used to further process exported data and eliminate compounds outside acceptable criteria. XIC hits were defined as having mass errors within ± 10 ppm, isotope ratio differences of <25%, and a spectral library match of <70% (analogous to confidence level 4 on scale defined by Schymanski et al.).³⁷ Library hits were defined as meeting XIC hit criteria while also having a spectral library match of >70% (analogous to confidence level 2).37 A protocol described by Nickerson et al.31 was then applied for semiquantitative analysis of suspect PFASs. Briefly, relevant ionizable groups from targeted analysis were assigned to suspect PFAS classes with similar ionizable groups and alkylchain fluorination.³¹ It is worth noting that semiquantification of zwitterions detected in ESI- mode using ESI- target calibrants may underestimate zwitterion semiquantitation values compared to using ESI+ target calibrants³¹ in ESI+ mode; only ESI⁻ mode analysis was performed in this study.

■ RESULTS AND DISCUSSION

Summary of Targeted Analysis of PFASs in AFFF. In a previous report, 14 UV-sulfite treatment was performed on an AFFF mixture diluted 1 to 60 000 in a pH-buffered sulfite sensitizer solution. Targeted analysis against a group of 44 reference standards revealed 15 PFASs with a total concentration of 93 μ g L⁻¹, including PFSAs (3C-9C), PFCAs (4C-8C), and FTSs (6C, 8C, and 10C). The total fluorine content of these analytes was 59 μ g of F L⁻¹, representing 37% of the total fluorine content of the AFFF estimated from ¹⁹F nuclear magnetic resonance (NMR) (162 μg of F L⁻¹). Furthermore, the total oxidizable precursor (TOP) assay showed generation of an additional 123 μ g of PFCAs per liter from precursors compared to the initial PFCA concentration (3.6 μ g L⁻¹). Thus, it follows that the AFFF contained a wide range of precursors and other PFASs not accounted for by targeted analysis of commonly monitored fluoroalkyl acids.

Suspect Analysis of PFASs in AFFF. Suspect screening analysis with LC-QTOF-MS revealed 68 additional PFASs detected throughout UV-sulfite treatment representing a wide range of structural classes (Table 1), with 23 of these PFASs showing at least one reaction time-course point with an MS/ MS spectral library match of >70% (Table S1); the remaining PFASs were identified solely as XIC hits. Structural isomers were reported when a single peak met XIC match criteria for more than one possible structure and a single structure could not be identified. Isomers were omitted if XIC hits contained library matches for a single structure in time-course samples. Reported PFASs include structures initially reported in or inferred from other work, 1,7,9,25,26,38-48 and combined with the 15 analytes detected by targeted analysis, a total of 83 PFASs were detected in the diluted AFFF throughout UV-sulfite treatment, spanning 32 classes and eight super classes (PFAS compound and class definitions listed in Table S2). Sorted by super class, 12 PFAAs, six FTSs and fluorotelomer carboxylic acids (FTCAs), eight FTS and FTCA derivatives, one fluorotelomer sulfonate/sulfate, three PFSA derivatives, 14 substituted PFAA derivatives, five cyclic and unsaturated PFAAs, and 34 sulfonamide precursors were detected throughout UV-sulfite treatment.

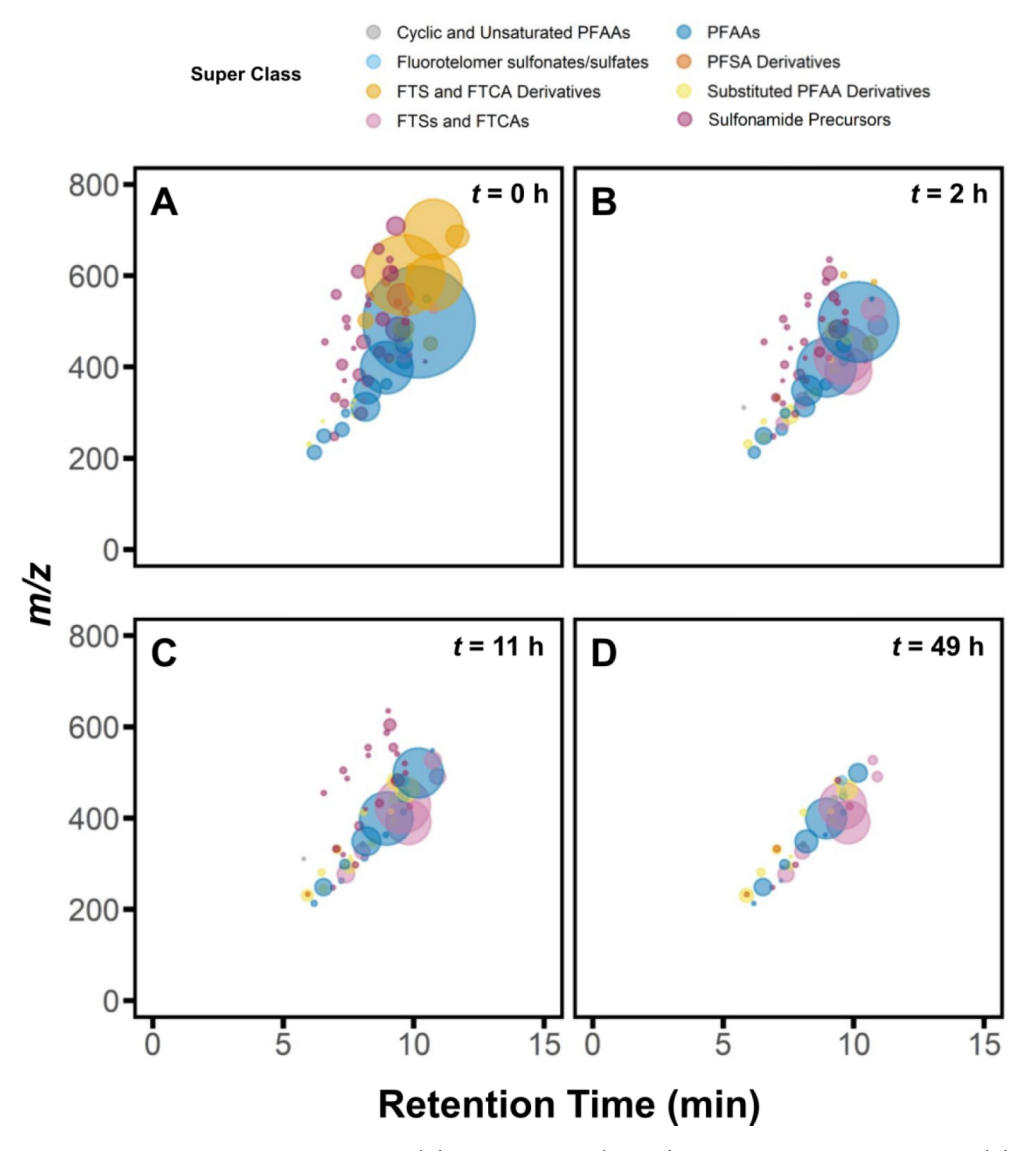


Figure 1. Quantitative and semiquantitative analysis of PFASs (A) before reaction (t = 0 h) and after UV-sulfite reaction for (B) 2 h, (C) 11 h, and (D) 49 h. Bubbles signify individual PFASs and are organized by PFAS super class indicated by color (see the legend). The area of each bubble is proportional to the concentration (micrograms per liter). The x-axis denotes the chromatographic retention time of the compound, and the y-axis denotes the mass-to-charge ratio (m/z) of the compound. Reaction time courses for individual PFASs detected by suspect screening analysis are provided in Figure S1; time courses for PFASs detected by targeted analysis were reported previously. The concentrations, semiquantitative concentrations, retention times, and m/z values were averaged from two replicates. Reaction conditions: AFFF (1 to 60 000 dilution in anoxic water), 10 mM Na₂SO₃, 5 mM NaHCO₃ buffer (pH₀ = 9.5), 20 °C, irradiation with an 18 W UV LP Hg lamp.

Semiquantitative analysis of suspect PFASs yielded a total of 74 μ g of PFASs per liter. Combined with the targeted analytes (93 μ g L⁻¹), a total of 167 μ g of PFASs per liter was estimated in the diluted AFFF. Thus, suspect screening analysis accounted for almost half (44%) of the total PFAS mass detected. Suspect analytes accounted for 32 μ g of F L⁻¹ or 20% of the total fluorine (total F = 162 μ g of F L⁻¹) in the diluted AFFF. Combined, 91 μ g of F L⁻¹, or 57% of the total fluorine, was accounted for by targeted and suspect screening analyses. This amount is smaller than the amount of fluorine accounted for after the TOP assay (125 μ g of F L⁻¹, 77% total fluorine). Still, given the greater uncertainty of semi-quantitative analysis, this represents a significant fraction of the fluorine mass balance in this complex mixture.

A majority of the PFASs detected were PFAAs (92 μ g L⁻¹, ~55% of total PFASs), consistent with their origination from an electrochemical fluorination manufacturing process that

produces a mixture of PFAAs. 9 All PFAAs were detected by targeted analysis, with PFOS accounting for the majority of the PFAA mass (75%) in the AFFF. 14 The second most abundant super class was the super class of FTS and FTCA derivatives, accounting for 60 μ g L⁻¹ or 36% of the total PFASs detected. Previously, it was shown that the unreacted AFFF contained small initial concentrations of 4:2, 6:2, and 8:2 FTS, but these increased >10-fold after UV-sulfite reaction for 2 h, 14 consistent with an abundance of fluorotelomer precursors. 1 The third most abundant super class consisted of sulfonamide precursors, accounting for 7% of the total PFASs detected (12 μ g L⁻¹). This is consistent with earlier reports of 3M AFFF formulations. As shown previously, perfluorooctanesulfonamidoacetic acid (FOSAA) can form PFAAs (e.g., PFOA and PFOS) during UV-sulfite treatment and could be a source for increases in selected PFAA concentrations observed at early UV-sulfite reaction time points. 14 This is plausible because

sulfonamide precursor concentrations (12 μ g L⁻¹) were ~3-fold greater than PFCA concentrations (3.6 μ g L⁻¹) in unreacted AFFF. The remaining super classes, including FTSs and FTCAs, fluorotelomer sulfonates/sulfates, substituted PFAA derivatives, and cyclic and unsaturated PFAAs, each represented <1% of total PFASs detected; PFSA derivatives were undetected in the unreacted AFFF and were observed only after UV-sulfite reactions had been initiated.

Evolution of PFAS Concentrations during UV-Sulfite Treatment. Figure 1 shows a series of "bubble" plots summarizing how concentrations of individual PFASs detected in the AFFF change as the UV-sulfite reaction proceeds. These plots arrange PFASs by their chromatographic retention time (x-axis) and mass-to-charge ratio (m/z, y-axis), with the diameter of each "bubble" being proportional to the estimated concentration of the analyte in question (organized by super class listed in Table 1). Full reaction time courses are provided in the Supporting Information for individual PFASs detected by suspect screening analysis (Figure S1). All reactions were performed for 49 h. Semiquantitative concentrations were displayed only for time points at which PFASs were detected; missing points indicate no detection at those times. Time courses for target PFAS analytes were reported previously. 14

Comparison of the plots before (Figure 1A) and after (Figure 1D) reaction shows an overall decrease in mass of the monitored analytes following treatment; PFAS concentrations collectively decreased by 79% after reaction for 49 h. This suggests an effective strategy for the treatment of AFFFimpacted water sources. Closer examination of the timedependent trends for individual analytes reveals differing behaviors that can be binned (Table 1) according to whether they were detected in the untreated AFFF (P, present; U, undetected), their tendency to initially increase in concentration during the first few hours of reaction before stabilizing or degrading (I, initially increases in concentration; O, no apparent initial increase in concentration), and whether the structure then degrades with further increases in reaction time (D, degrades; R, recalcitrant). For example, an analyte that is initially present in the AFFF but increases in concentration over the first 2 h of reaction before reaching a maximum concentration and then decreasing over the remaining time period monitored is binned as "P-I-D".

PFAS Generation. Panels B and C of Figure 1 show bubble plots, including the 30 compounds that were generated (Table 1, bin I), for the 2 and 11 h time points, respectively. Comparing panels B and C with panel D shows that while many structures were removed after reaction for 49 h, observing intermediate time points (t = 2 and 11 h) shows that some structures were generated during early stages of treatment. Reaction time courses (Figure S1) also show that selected PFASs were generated within the first 11 h of reaction. This is consistent with earlier work showing that UV-sulfite treatment of FOSAA led to generation of PFOS, PFOA, and perfluorooctane sulfonamide (FOSA) within the first hour of reaction. ¹⁴

$$\begin{array}{c} \underset{F}{\text{F}} \underset{F}{\text{F}} \underset{F}{\text{F}} \underset{F}{\text{F}} \underset{F}{\text{F}} \underset{O}{\text{H}} \xrightarrow{\text{O}} \xrightarrow{\text{O}} \xrightarrow{\text{O}} \xrightarrow{\text{O}} \xrightarrow{\text{O}} \xrightarrow{\text{O}} \xrightarrow{\text{F}} \xrightarrow{\text{F}} \underset{F}{\text{F}} \underset{F}{\text{F}} \xrightarrow{\text{F}} \xrightarrow{\text{F}} \xrightarrow{\text{F}} \xrightarrow{\text{O}} \xrightarrow{\text{O}$$

Eighty-three total target and suspect compounds were detected throughout the course of UV-sulfite experiments, with the diversity of PFASs detected evolving with reaction time. While 69 target and suspect compounds were detected

before reaction, 75 compounds were detected at 0.5 h, 68 at 2 h, 60 at 11 h, and 37 at 49 h. This indicates that (i) 14 PFASs were undetected in unreacted AFFF (Table 1, bin U) and generated during UV-sulfite treatment, (ii) undetected PFASs in unreacted AFFF appear after reaction for 2 or 11 h while others disappear over the same time period, and (iii) more than half (55%) of the PFASs in this AFFF were degraded below detection after treatment for 49 h. Thus, the evolution of PFAS composition during the UV-sulfite treatment of AFFF is complex, involving both formation and degradation of individual PFASs within the suspect screening list. When fluorotelomer sulfonates/sulfates were excluded, PFASs from each super class were generated during the early stages of UVsulfite treatment. Almost all substituted PFAA derivatives (11 of 14) were photogenerated (Table 1, bin I) while only one of 34 sulfonamide precursors and two of nine FTS and FTCA derivatives were photogenerated. Instead, reaction of e_{aq}^{-} with nonphotogenerated structures (Table 1, bin O) may be sources of formation of other structures that are observed to increase in concentration during early phases of reaction (discussed below). Analytes that increased in concentration during the early phases of the reaction fell into the lowermolecular weight range (m/z 231-527) of structures identified (full range, m/z 214–710). This is suggestive of reaction pathways in which e_{aq} reactions cleave bonds within the backbone of higher-molecular weight precursors (e.g., cleavage of the S-N bond at the tertiary amine in the diOHPrAm-MeOHPr-FASAPrS class could generate PFSAs):

diOHPrAm-MeOHPr-FASAPrS

PESA

PFAS Degradation. Concentrations of 65 PFASs degraded by >50% from their maximum values (Table 1, bin D) during the time monitored. For 39 of these, degradation kinetics followed a pseudo-first-order rate law, allowing for estimates of the pseudo-first-order rate constants for degradation (k_{obs}) inverse hours) and reaction half-lives ($t_{1/2}$, hours). As described previously, ¹⁴ $k_{\rm obs}$ values for PFASs exhibiting generation were estimated using data points following the time of maximum concentration. Values were also estimated for 13 compounds containing only two or three points in their time courses and a one-point lower bound $k_{\rm obs}$ estimate¹⁴ for 8:2 FTTh-PrAd-DiMeEtS assuming a concentration of 0 μ g L⁻¹ at 0.5 h. Degradation of the 11 remaining compounds did not follow apparent first-order behavior, but $t_{1/2}$ values were estimated by interpolation of time-course data. Due to the low initial concentration (0.01 μ g L⁻¹), CMeAmPr-FBSA was detected for only the first 2 h (maximum 35% degradation). Thus, $t_{1/2}$ was estimated by extrapolating from linear regression of observed non-first-order decay. The lack of first-order decay could be due to (1) few time-course data points due to sharp decay falling below detection levels, (2) scatter due to poor detection caused by low concentrations, or (3) non-first-order sharp declines in concentration. It is worth noting that sulfite concentrations decrease slowly during UV reactions, but >30% of the initial concentration remained after irradiation for 49 h. 14 This is not expected to appreciably affect the measured $k_{\rm obs}$ and $t_{1/2}$ values for most PFASs in the AFFF mixture, especially those for which $t_{1/2} \le 12$ h (78% of reactive PFASs)

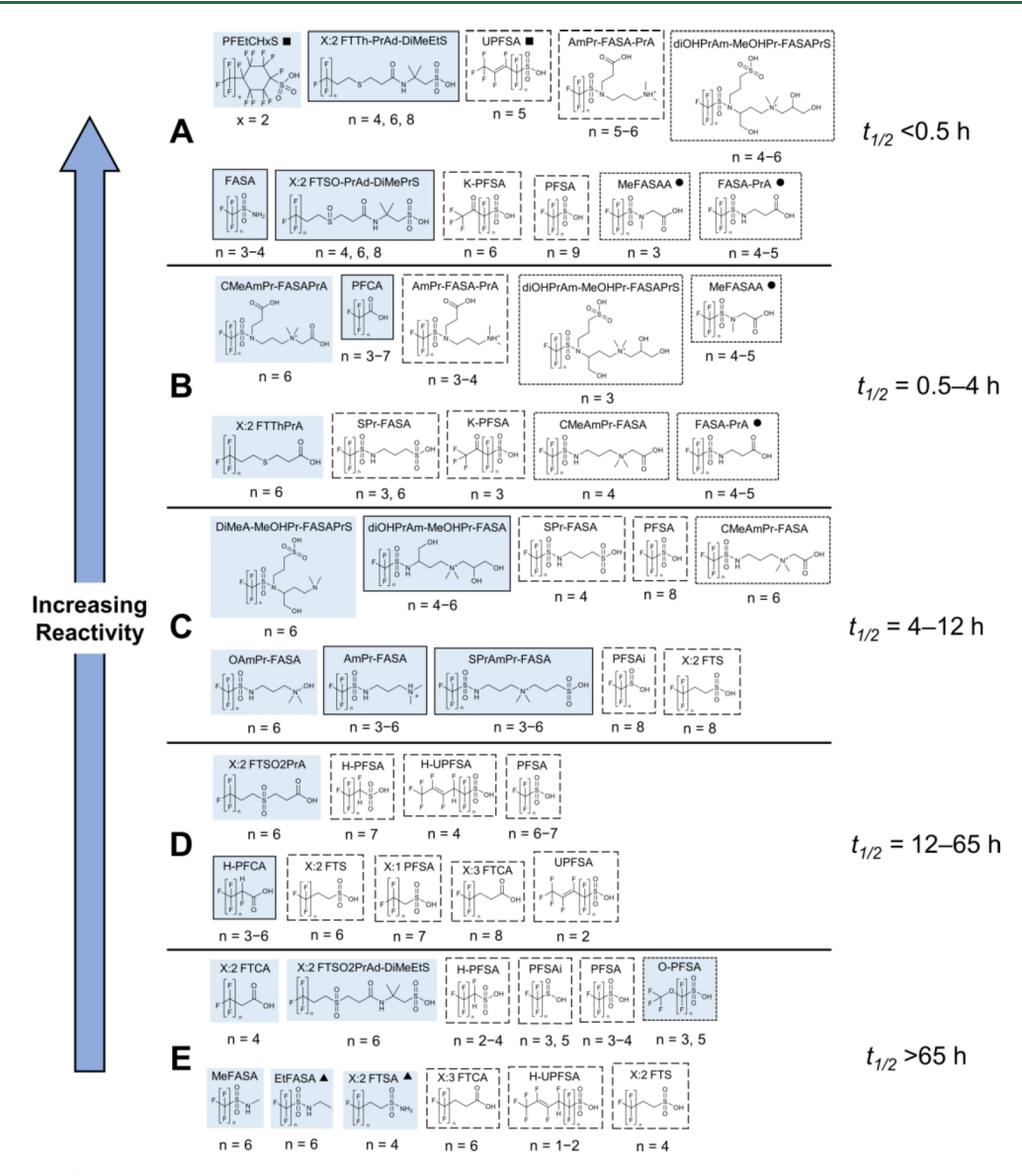


Figure 2. Half-lives $(t_{1/2})$ of PFASs observed during UV-sulfite treatment. Sections are organized by apparent reactivity: compounds with $t_{1/2}$ values of (A) 0–0.5 h, (B) 0.5–4 h, (C) 4–12 h, (D) 12–65 h, and (E) >65 h. Shaded classes appear exclusively in one $t_{1/2}$ range (no border indicates a single PFAS in the class). Solid borders indicate classes that appear in multiple $t_{1/2}$ ranges and are independent of chain length. Long-dash borders indicate classes that appear in multiple $t_{1/2}$ ranges and are dependent on chain length. Dotted borders indicate classes with special case chain length reactivity trends. Half-life values for individual compounds are provided in Figure S2. Matching symbols indicate structural isomers.

because sulfite concentrations remained high over this time period. Still, it is worth noting that the measured rate constants for the most recalcitrant PFASs may be slight underestimates due to the effects of decreasing sulfite concentration over the course of extended reaction times. Figure 2 summarizes the estimated half-lives for 65 PFASs organized by apparent reactivities.

Highly reactive PFASs $(t_{1/2} < 0.5 \text{ h})$ contained reduced sulfur groups adjacent to the fluorotelomer $[F(CF_2)_n(CH_2)_2-]$ chain. X:2 FTTh-PrAd-DiMeEtS and X:2 FTSO-PrAd-DiMePrS classes have thioether (-S-) and sulfinyl (-SO-) adjacent to the $F(CF_2)_n(CH_2)_2-$ chain and share propanamido dimethyl ethyl sulfonate moieties in the headgroup (Figure 2A). The X:2 FTSO2PrAd-DiMeEtS class, with a similar propanoamido dimethyl ethyl sulfonate headgroup, was much more recalcitrant and contained a more oxidized sulfonyl group $(-SO_2-)$ adjacent to the $F(CF_2)_n(CH_2)_2-$ chain (Figure 2E). Previous reports indicate that amino acids

containing -S-S-, -S-, and -SH groups are highly reactive with e_{aq}^{-} (10^8-10^{10} M $^{-1}$ s $^{-1}$) and -S-S- and -SH are known sites of e_{aq}^{-} attack; 49,50 however, the rate constant for dimethyl sulfoxide (containing -SO-) is on the order of only $\sim 10^6$ M $^{-1}$ s $^{-1,20}$ Rather than being a site of attack, -SO- adjacent to the $F(CF_2)_n(CH_2)_2-$ chain may instead influence C-F release and reactivity. Other work has shown that low bond dissociation energies (BDEs) of C-F bonds on carbon atoms in the α position relative to the carboxylate headgroup contributed to the high reactivity of PFCAs, whereas higher BDEs of C-F bonds on the α carbons in PFSAs contributed to their greater recalcitrance. Additionally, high concentrations of highly reactive FTS and FTCA derivatives (59 μ g L $^{-1}$, X:2 FTSO-PrAd-DiMePrS and X:2 FTTh-PrAd-DiMeEtS combined) in this AFFF could be the source of FTS formation during UV-sulfite reactions reported previously (discussed below). In the content of the cont

Exceptions to the low reactivity of more oxidized sulfur groups include PFNS, which had $k_{\rm obs}$ values that were much greater than those of shorter-chain PFSAs, possibly an artifact due to estimation from only two available data points.¹⁴ UPFOS, containing an unsaturated bond, was also highly reactive. While the unsaturated bond could induce higher reactivity, PFEtCHxS, the UPFOS isomer, and its cyclic structure could instead react with e_{aq}-. One report found significant reduction catalyzed degradation (~70%) of a carboxylic acid analogue of CHxS by cobalt catalysts; low BDEs of tertiary C-F bonds within this structure led to a proposed mechanism involving defluorination at this tertiary C-F bond. 51 K-PFOS is highly reactive, likely due to the ketone moiety; ketones are known quenchers of e_{aq} - ⁵² Higher reactivity in K-PFOS could also suggest ketone moieties impact the reactivity of adjacent C-F bonds, similar to a headgroup. Bentel and co-workers found that dicarboxylic acids had C-F bonds with lower BDEs at carbons adjacent to both carboxylic acid headgroups, contributing to higher reactivity.15

Primary and tertiary sulfonamides also appear to have high reactivity with $e_{aq}^{}$ and compose almost half of all PFASs with $t_{1/2}$ values of <0.5 h. While reported second-order rate constants of alkyl chains containing primary amines are low $(10^5-10^6 \text{ M}^{-1} \text{ s}^{-1})$, 20,49 the high reactivity of short-chain terminal primary sulfonamides [-SO₂NH₂ (Figure 2A)] compared to short-chain terminal sulfonate groups [-SO₃ (Figure 2E)] may indicate the primary sulfonamide induces high reactivity in FASAs either by direct reaction at the amine or by influencing C-F release along the perfluoroalkyl $[F(CF_2)_n-]$ chain similar to the carboxylic acid in PFCAs. Previous studies have shown aliphatic amino acids are highly reactive with e_{aq}^{-} (10⁸-10⁹ M⁻¹ s⁻¹), with the carbonyl being the reaction site and leading to deamination, 50,53 which contrasts with lower reactivity of aliphatic carboxylic acids (106 M⁻¹ s⁻¹)⁵⁴ or alkyl amines. ²⁰ This suggests that amine moieties near the $F(CF_2)_n$ - chain may play an important role in PFAS reactivity.

PFCAs were the most reactive class identified by targeted analysis and were in the $t_{1/2} = 0.5-4$ h reactivity range. Reactivity increased with perfluorinated chain length for certain homologues, suggesting chain length-dependent reactivity (discussed below). Longer-chain PFSAs (e.g., PFOS) and FTSs (e.g., 8:2 FTS) identified by targeted analysis had reactivity in this intermediate range. Half of the most reactive PFASs ($t_{1/2}$ < 4 h) were sulfonamide precursors, and UV-sulfite reaction could lead to PFAA production as shown previously for FOSAA.¹⁴ In addition to tertiary sulfonamides, secondary sulfonamides (e.g., SPr-FASA and CMeAmPr-FBSA) had $t_{1/2}$ values of 0.5-4 h, suggesting that sulfonamides with varying amine types are highly susceptible to e_{aq} reaction. Additionally, sulfonamide precursors with secondary or tertiary amines were generally more reactive and exclusively had $t_{1/2}$ values of <12 h. It is unlikely that the lower reactivity for secondary and tertiary sulfonamides with $t_{1/2}$ values of 4–12 h can be explained by differences in specific moieties on the nonfluorinated headgroup. Generally, saturated carbon atoms are unreactive or have little reactivity with e_{aq}, but some features on nonfluorinated PFAS headgroups can be reactive with e_{aq}^- , including quaternary amines, amides $(-\text{CONH}_2)$, and amino acids. Additionally, charge has been shown to impact reactivity in amino acids. The reactivity of positively charged amino acid species with

protonated amine groups can be orders of magnitude higher than for the corresponding neutral or negatively charged species. However, PFASs containing these select functional groups or positively charged moieties were at times unreactive [e.g., 6:2 FTSO2PrAd-DiMeEtS (Figure 2E)] or exhibited chain length dependence (discussed below) and thus are not likely sites of e_{aq}^- attack. These results suggest moieties on the nonfluorinated headgroup positioned away from the $F(CF_2)_n - F(CF_2)_n (CH_2)_2 - Chain$ may influence C-F bond reactivity similar to carboxylic acids in PFCAs¹⁵ or S-N bond reactivity in sulfonamides adjacent to the $F(CF_2)_n - F(CF_2)_n - F(C$

Still lower reactivity was observed for PFASs in the substituted PFAA derivative, cyclic and unsaturated PFAA, and fluorotelomer sulfonate/sulfate super classes, which almost exclusively had $t_{1/2}$ values of 12–65 h (Figure 2D) or were unreactive on the time scale monitored. Unreactive PFASs were assigned a $t_{1/2}$ of >65 h (Figure 2E). The addition of more bonds to hydrogen along the $F(CF_2)_n$ – chain in PFAAs, including single-H substitution (e.g., H-PFSA and H-PFCA) and multiple-H substitution (e.g., X:1 PFSA, X:3 FTCA, and X:2 FTS), considerably decreased reactivity, as was observed in previous reports of UV-sulfite with individual target analytes and reaction product peak areas. 14,15 The decreased reactivity is sensitive to the position of H substitution; a hydrido group at the last carbon in ω -hydroperfluorocarboxylates (ω -HFPCAs) showed reactivity similar to that of PFCAs $(n \ge n)$ 3).²⁴ Substitution of an ether bond along the perfluorinated chain in the O-PFSA class also decreased reactivity. Previous work investigating UV-sulfite treatment of perfluoroalkyl ether carboxylic acids also showed that ether substitutions along the $F(CF_2)_n$ - chain decreased reactivity compared to fully perfluorinated PFCAs. 16 Structures including sulfonyl groups $(-SO_2-)$ adjacent to the $F(CF_2)_n(CH_2)_2$ chain (X:2)FTSO2PrA and X:2 FTSO2PrAd-DiMeEtS classes) were also unreactive. The addition of a smaller methyl or ethyl group adjacent to the sulfonamide headgroup in MeFHxSA and EtFHxSA decreased the reactivity of FASAs considerably, and these were the least reactive sulfonamides observed when compared with larger more complex headgroups of other sulfonamides. This further suggests that reactivity of sulfonamides (potentially at the S–N bond or C–F bonds) is greatly impacted by headgroup moieties adjacent to the sulfonamide. Alternatively, because 6:2 FTSA was an isomer of EtFHxA and a single structure could not be identified, this could instead suggest CH_2 groups between the $F(CF_2)_n$ chain and sulfonamide headgroup decrease sulfonamide reactivity. The remaining short-chain PFSAs and FTSs identified in targeted analysis were also in this recalcitrant range, consistent with the chain length reactivity dependence observed previously. 14 UPFPeS was also less reactive than the long-chain homologue, UPFOS.

Figure 2 also demonstrates that EPA standard methods of analysis that would be required by regulators during field deployments (e.g., U.S. EPA Methods 533 and 537.1) can be expected to capture the general effectiveness of a given UV-sulfite treatment system. Common PFAS target analytes in these methods (e.g., PFOA to PFBS) span most of the full reactivity range observed among target and suspect analytes [i.e., $t_{1/2} = 1$ to >65 h (Figure 2B–E)]. If degradation of target analytes with $t_{1/2}$ values of ~1 h is observed, one would expect that PFASs with $t_{1/2}$ values of <0.5 h will also be degraded.

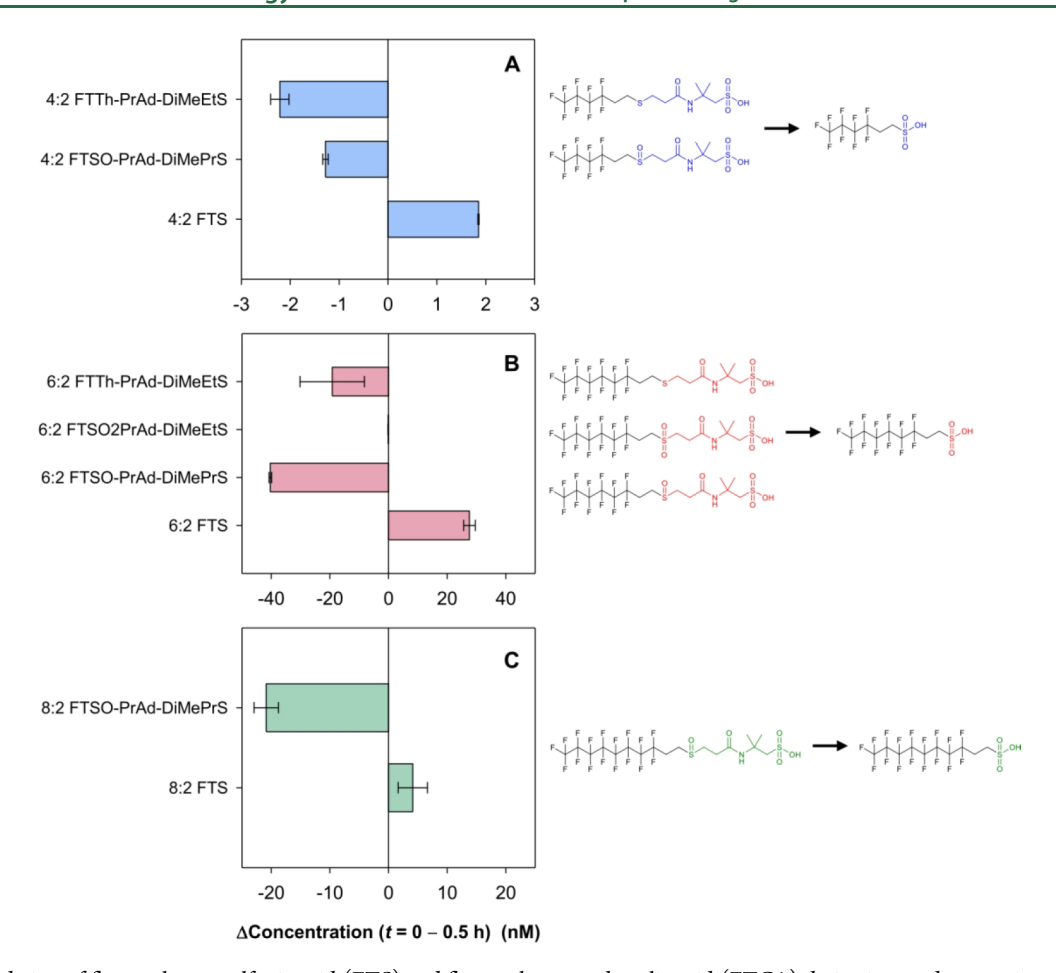


Figure 3. Degradation of fluorotelomer sulfonic acid (FTS) and fluorotelomer carboxylic acid (FTCA) derivatives and generation of fluorotelomer sulfonic acids (FTSs) with analogous (A) 4:2, (B) 6:2, and (C) 8:2 fluorotelomer chains after UV-sulfite reaction for 0.5 h. Error bars extend to minimum and maximum values observed in replicate reactions. Relevant chemical structures are presented at the right. Highlighted functional groups identify potential sites of conversion.

Generation of FTS from Fluorotelomer Derivative **Conversion.** We previously showed that 4:2, 6:2, and 8:2 FTSs (target analytes) were generated at concentrations >10fold higher than initial concentrations in the AFFF within the first 2 h of UV-sulfite treatment. 14 It was hypothesized that the generated FTSs were end products from reactions between $e_{aq}^{}$ and fluorotelomer acid precursors. Figure 3 compares the decay of fluorotelomer derivatives containing analogous X:2 fluorotelomer moieties with the formation of 4:2, 6:2, and 8:2 FTSs after reaction for 0.5 h on a molar basis. Over the first 0.5 h, 3.5 nM 4:2 fluorotelomer derivatives were degraded while 1.9 nM 4:2 FTS was generated (Figure 3A). Because the total molar concentration of degraded precursors was similar to that of 4:2 FTS formed, this suggests either 4:2 fluorotelomer derivatives are efficiently converted to 4:2 FTS or there are other unidentified precursors being converted to 4:2 FTS. Because the 60 nM 6:2 fluorotelomer derivative decay was 2fold greater than 6:2 FTS formation (Figure 3B), it is possible these derivatives were also precursors to 6:2 FTS generation.; 21 nM 8:2 fluorotelomer derivatives were degraded, while 4 nM 8:2 FTS was formed (Figure 3C). Because 8:2 FTSO-PrAd-DiMePrS decay was 5-fold greater than 8:2 FTS formation, it is also plausible that 8:2 FTSO-PrAd-DiMePrS is the major precursor of 8:2 FTS. While comparisons between losses of abundant precursors with corresponding FTS formations may help predict the origin of PFAS formation,

detailed mechanisms for these conversions remain unknown, and focused experiments using single precursor molecules are needed to elucidate reaction pathways. Previous results showed conversion of FOSAA to PFOS and PFOA.¹⁴ Similar to cleavage of the S-N bond in FOSAA, cleavage at the S-C bonds of S groups adjacent to $F(CF_2)_n(CH_2)_2$ - chains of FTS and FTCA derivatives may lead to FTS formation. Reaction mechanisms require oxidation of the thioether (-S-) or sulfonyl (-SO₂-) group to a terminal sulfonate group (-SO₃⁻). One study showed that 6:2 FTS was a major product of 6:2 FTTh-PrAd-DiMeEtS via aerobic biotransformation in AFFF-impacted soil slurries enriched with an Ansul formulation.⁵⁶ Analysis of product ions suggested addition of one or two oxygen atoms to the sulfur in the fluorotelomer thioether group. 66 A similar abiotic transformation pathway has been observed during soil extraction.³¹

Influence of Chain Length. Figure 2 shows certain PFAS classes detected by suspect screening analysis spanned multiple $t_{1/2}$ ranges due to chain length-dependent reactivity already noted for both PFSAs and FTSs, where reactivity increases with chain length. Half-lives for PFAS classes detected in suspect screening analysis having chain length-dependent reactivity are summarized in Figure S3. Multiple classes of sulfonic acids (e.g., perfluoroalkyl, H— and ketone-substituted, and unsaturated), sulfinates (terminal $-SO_2^-$), fluorotelomer acids (sulfonic and carboxylic), and tertiary sulfonamides

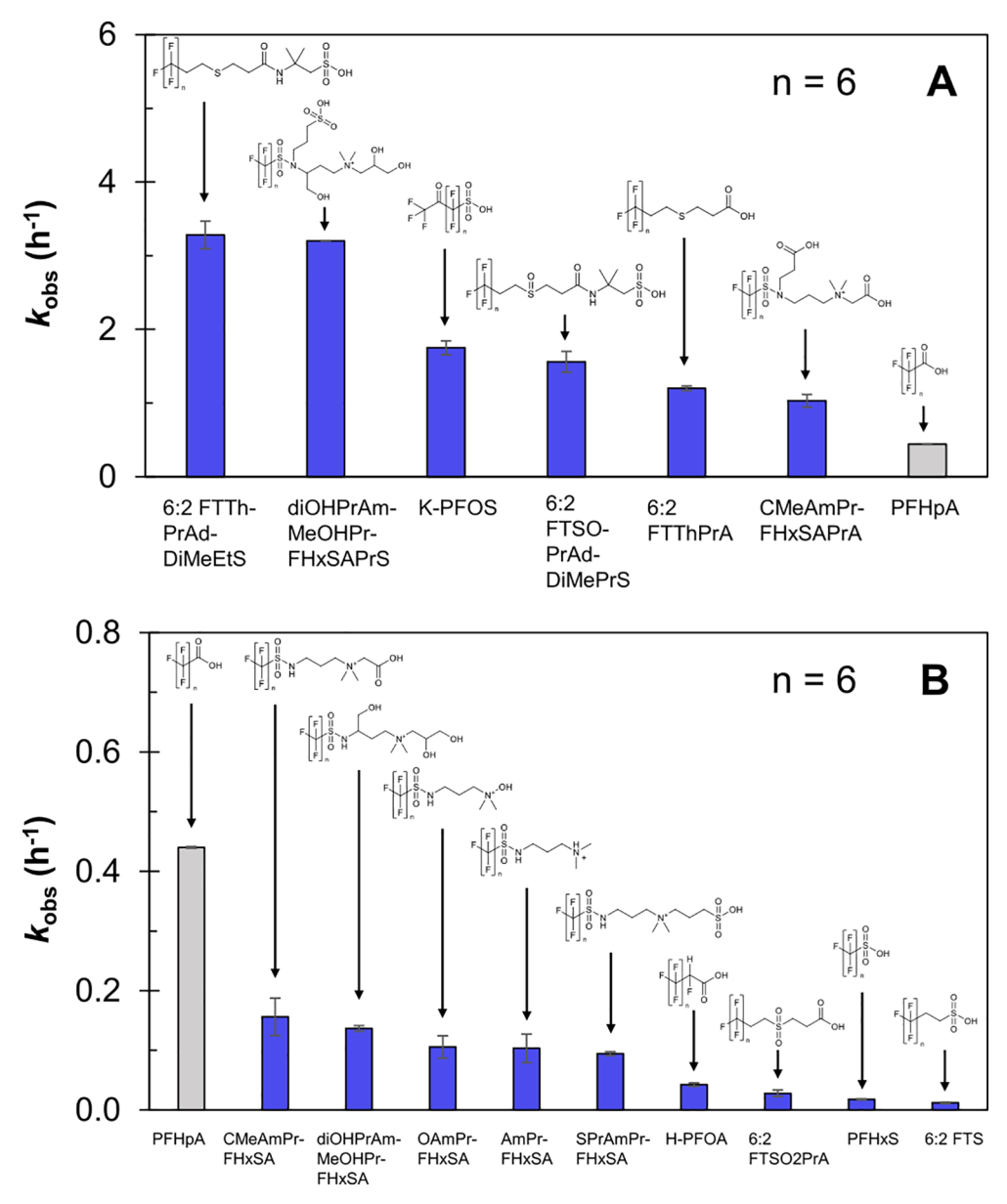


Figure 4. Comparison of apparent first-order rate constants (k_{obs}) for degradation of PFASs with six repeating CF₂ groups (n = 6) from different structural classes during UV-sulfite treatment. Structures are arranged in two groups: (A) PFASs with k_{obs} values exceeding the value measured for n = 6 PFCA (PFHpA; shown as a gray bar in both panels) and (B) PFASs with k_{obs} values lower than the value measured for PFHpA.

exhibited chain length-dependent reactivity patterns. Because PFEtCHxS is an isomer of UPFOS and a single structure could not be identified, it is possible only UPFPeS was identified and UPFSA reactivity trends were not observed. Previous reports have shown that headgroup moieties adjacent to the $F(CF_2)_n$ chain induce chain length dependence in PFASs by affecting the BDEs of C-F bonds along the $F(CF_2)_n$ - alkyl chain. Chain length dependence was explained by weaker BDEs in C-F bonds near the middle of $F(CF_2)_n$ chains in longerchain PFASs compared to higher BDEs near the headgroup and near the terminal -CF₃ group. 15 The amine type (e.g., tertiary amine) and sulfur group oxidation state (e.g., $-SO_2^$ and $-SO_3^-$) adjacent to $F(CF_2)_n - /F(CF_2)_n (CH_2)_2 -$ chains may also induce similar chain length effects on reactivity. Chain length dependence for fluorotelomer acids is consistent with recent reports of UV-sulfite reactivity with individual carboxylic acids, where substitution of multiple H's for F (i.e., -CF₂CF₂- with -CH₂CH₂-) near the terminal carboxylate

headgroup introduced chain length-dependent reactivity that was not apparent for fully fluorinated PFCAs.¹⁵

In contrast to PFSAs and FTSs, we previously noted that the reactivity of PFCAs was relatively independent of chain length in diluted AFFF. 14 This is also true for multiple PFAS classes detected by suspect screening analysis (Figure 2). The $t_{1/2}$ values for classes with chain length-independent reactivity are presented in Figure S4. While FTCAs showed chain lengthdependent reactivity, this did not extend to H-PFCAs even though both contain H substitution along the $F(CF_2)_n$ - chain. Though the position of H substitution is known for FTCAs (i.e., adjacent to the carboxylic acid), it is unknown for H-PFCAs because multiple isomers are possible. Differences in chain length-dependent versus -independent reactivity could suggest H-PFCAs in this study had H substitution away from the carboxylic acid group, leading to chain length-independent reactivity. A recent report also showed H substitution at the last carbon in ω-HPFCAs maintained chain length-independent trends for PFCAs with $n \ge 3$.²⁴ Sulfonamides with primary or secondary amines adjacent to the $F(CF_2)_n$ — chain also displayed chain length-independent reactivity. High reactivity and chain length independence of primary and secondary sulfonamides may suggest primary and secondary sulfonamides share a specific site of e_{aq}^- attack.

Special case chain length reactivity trends are presented in Figure S5. The reactivity increased with a decrease in chain length for X:2 FTTh-PrAd-DiMeEtS and MeFASAA classes. MeFASAAs are isomers of recently identified FASA-PrAs; ⁵⁷ thus, a single class structure could not be identified. This trend was not observed for any other classes in targeted or suspect screening analysis, nor has it been reported previously. The O-PFSA class was unreactive for all chain lengths observed. Because a $t_{1/2}$ of >65 h was observed for 5C and 7C homologues, it was not possible to determine a chain length reactivity trend.

Influence of Polar Functional Groups. Acquisition of substantial PFAS information across a wide array of classes allows for reactivity comparisons among structures having common numbers of repeating CF_2 groups (i.e., n) but varying in class (e.g., perfluoroalkyl vs fluorotelomer), $F(CF_2)_n$ – chain substitution, and headgroup identity. Figure 4 compares $k_{\rm obs}$ values for PFASs with n = 6 from different classes; the n = 6PFCA (PFHpA) was used as a reference for reactivity. It should be noted that 6:2 FTThPrA, PFHpA, H-PFOA, PFHxS, and 6:2 FTS were all photogenerated (Table 1). Simultaneous formation and degradation could bias rate constants low depending on the respective precursor concentrations of each PFAS (unknown at this time), as mentioned previously. ¹⁴ FTS and FTCA derivatives (e.g., 6:2 FTTh-PrAd-DiMeEtS, 6:2 FTSO-PrAd-DiMePrS, and 6:2 FTThPrA), sulfonamide precursors (e.g., diOHPrAm-MeOHPr-FHxSA and CMeAmPr-FHxSAPrA), and a substituted PFAA derivative (K-PFOS) were 2–8 times more reactive than PFHpA (Figure 4A). As discussed previously, reduced sulfur groups adjacent to the $F(CF_2)_n(CH_2)_2$ - chain may increase the reactivity of PFASs by being a site of attack (e.g., -S-) or impacting C-F bond reactivity (e.g., -SO-), high reactivity was observed for tertiary amines in this study, and ketones in K-PFSA could explain high reactivity.⁵²

A majority of the PFASs that were less reactive than PFHpA (Figure 4B) were sulfonamide precursors containing secondary sulfonamides. The $k_{\rm obs}$ for PFHpA was 3–5 times greater than the $k_{\rm obs}$ of sulfonamide precursors. The lowest reactivity was exhibited by PFASs with more oxidized sulfur groups (e.g., $-SO_2$ and $-SO_3$ adjacent to the $F(CF_2)_n$ or F- $(CF_2)_n(CH_2)_2$ - chain. Alkyl compounds containing highly oxidized sulfur groups (e.g., -SO₃⁻ and -OSO₃⁻) tend to have lower second-order rate constants with e_{aq}^{-} (10⁶-10⁷ M⁻¹ s⁻¹).²⁰ Additionally, these oxidized sulfur groups may decrease the reactivity of C-F bonds along the $F(CF_2)_n$ or $F(CF_2)_n(CH_2)_2$ - chain similar to PFSAs. 15 Replacement of fluorine with H adjacent to the sulfonate headgroup in fluorotelomers dramatically inhibits reaction (e.g., 6:2 FTS). Additionally, H substitution in H-PFOA decreased the reactivity 10-fold compared with that of PFHpA. The decreased reactivity with H substitution was also observed for carboxylic acids by Bentel and co-workers. 15 As mentioned previously, ω -HPFCAs (H- at the last fluorocarbon) showed reactivity similar to that of PFCAs,²⁴ suggesting the hydrido group was not at the end fluorocarbon of H-PFOA in this study.

Environmental Implications. This work demonstrates that application of suspect screening and semiquantitative analysis can be used to monitor reactions of PFAS mixtures during treatment processes, enabling the tracking of the formation and decay of individual PFASs. Co-contaminants and geochemistry may pose challenges to detection and recovery in real AFFF-impacted waters due to suppression caused by the matrix. Reviewing internal standard recovery data (information available using methods in this study) in real matrices and comparing with recovery in a clean matrix may be necessary to assess impacts of matrix effects. While much research has focused on the transformation of PFAA precursors to PFAAs via chemical/biological oxidation, 10,38,58-60 this work shows for the first time that high concentrations of highly reactive longer-chain FTS and FTCA precursors and sulfonamide precursors may transform into shorter-chain PFAAs and FTSs via UV-sulfite-initiated reactions, generating concentrations of these acids higher than those initially present in AFFF. Some of these structures are recalcitrant end products that will persist following their formation. Reactions with precursors must be considered, and precursor concentrations should be monitored by applying broader PFAS analytical methods before applying UV-sulfite treatment, particularly the more reactive sulfonamide precursors containing primary and tertiary sulfonamide groups (e.g., $-SO_2N-$) adjacent to the $F(CF_2)_n$ chain (e.g., FASA) and AmPr-FASA-PrA classes) and FTS and FTCA precursors containing reduced sulfur groups (e.g., -S- and -SO-) adjacent to the $F(CF_2)_n(CH_2)_2$ - chain (e.g., X:2 FTTh-PrAd-DiMeEtS and X:2 FTSO-PrAd-DiMePrS classes). Failure to account for the presence of precursors during UV-sulfite treatment of AFFF-impacted waters could result in the generation of highly recalcitrant end products (e.g., PFAAs and FTSs) limiting destructive treatment. Additionally, H substitution, ether substitution, fluorotelomer moieties, and more oxidized sulfur groups adjacent to the $F(CF_2)_n$ or $F(CF_2)_n(CH_2)_2$ - chain (e.g., $-SO_2$ - and $-SO_3$) introduced more recalcitrance in acids and may create challenges for UVsulfite remediation in addition to the increased level of substitution of less reactive/unreactive shorter-chain homologues. 61 Monitoring PFAS classes containing these recalcitrant functional groups may be a useful indicator for determining effective PFAS treatment if present in waters. PFSAs, fluorotelomer acids, tertiary sulfonamides, H-substituted PFASs, and sulfinates exhibited chain length-dependent reactivity, while PFCAs, sulfoxides, H-PFCAs, and primary and secondary sulfonamides show chain length-independent reactivity. Thus, the character of the group adjacent to the $F(CF_2)_n$ or $F(CF_2)_n(CH_2)_2$ chain (e.g., sulfur group oxidation state, sulfonamide type, and carboxylic acid) and substitution along the $F(CF_2)_n$ or $F(CF_2)_n(CH_2)_2$ chain (e.g., H, ketone, and ether) combine to impact PFAS reactivity trends.

Future work should focus on understanding PFAS reactivity in AFFF-impacted groundwaters. The results from this study suggest natural precursor transformation processes (e.g., biological and chemical) in groundwater may alleviate issues caused by the conversion of reductive precursors to perfluoroalkyl and fluorotelomer acids. Oxidative pretreatment (e.g., advanced oxidation processes) could serve as a proxy for natural precursor transformation in fresh AFFF spills to convert precursors and fluorotelomers predominantly to more highly reactive and chain length-independent PFCAs, similar

to recent work using fluorotelomer acids, ²³ mitigating this issue.

ASSOCIATED CONTENT

Supporting Information

The Supporting Information is available free of charge at https://pubs.acs.org/doi/10.1021/acs.est.2c03228.

A list of chemical reagents, PFAS reaction time courses, a list of library matches, PFAS names, graphical presentation of $t_{1/2}$ ranges and reactivity trends, and a list of structural isomers (PDF)

AUTHOR INFORMATION

Corresponding Author

Timothy J. Strathmann — Department of Civil and Environmental Engineering, Colorado School of Mines, Golden, Colorado 80401, United States; orcid.org/0000-0002-7299-3115; Phone: (303) 384-2226; Email: strthmnn@mines.edu

Authors

Raul Tenorio — Department of Civil and Environmental Engineering, University of Illinois at Urbana-Champaign, Urbana, Illinois 61801, United States; Department of Civil and Environmental Engineering, Colorado School of Mines, Golden, Colorado 80401, United States; Present Address: R.T.: Haley & Aldrich, 400 E. Van Buren St., #545, Phoenix, AZ 85004; orcid.org/0000-0001-9788-7100

Andrew C. Maizel — Department of Civil and Environmental Engineering, Colorado School of Mines, Golden, Colorado 80401, United States; Institute for Soft Matter Synthesis and Metrology, Georgetown University, Washington, D.C. 20057, United States; orcid.org/0000-0002-2981-5241

Charles E. Schaefer – CDM Smith, Edison, New Jersey 08837, United States; orcid.org/0000-0003-4141-0148 Christopher P. Higgins – Department of Civil and

Environmental Engineering, Colorado School of Mines, Golden, Colorado 80401, United States; orcid.org/0000-0001-6220-8673

Complete contact information is available at: https://pubs.acs.org/10.1021/acs.est.2c03228

Notes

The authors declare no competing financial interest.

ACKNOWLEDGMENTS

This work was supported by the Strategic Environmental Research and Development Program (SERDP, Grant ER-2424), the Air Force Civil Engineering Center (AFCEC, Grant BAA-031), and the National Science Foundation (CHE Award 1807739). The authors also acknowledge the NSF GRFP (Grant DGE-1746047), the Support for Under-Represented Groups in Engineering (SURGE) Fellowship Program (UIUC), and a Civil and Environmental Engineering Distinguished Fellowship (UIUC) for the financial support of R.T. The authors also thank Youn-Jeong Choi, Sydney Binette, and Anastasia Nickerson for assistance with the LC-QTOF-MS and discussions about semiquantitative analysis.

REFERENCES

- (1) Place, B. J.; Field, J. A. Identification of Novel Fluorochemicals in Aqueous Film-Forming Foams Used by the US Military. *Environ. Sci. Technol.* **2012**, *46*, 7120–7127.
- (2) Ahrens, L.; Norström, K.; Viktor, T.; Cousins, A. P.; Josefsson, S. Stockholm Arlanda Airport as a Source of Per- and Polyfluoroalkyl Substances to Water, Sediment and Fish. *Chemosphere* **2015**, *129*, 33–38
- (3) Moody, C. A.; Hebert, G. N.; Strauss, S. H.; Field, J. A. Occurrence and Persistence of Perfluorooctanesulfonate and Other Perfluorinated Surfactants in Groundwater at a Fire-Training Area at Wurtsmith Air Force Base, Michigan, USA. *J. Environ. Monit.* **2003**, *S*, 341–345
- (4) Hu, X. C.; Andrews, D. Q.; Lindstrom, A. B.; Bruton, T. A.; Schaider, L. A.; Grandjean, P.; Lohmann, R.; Carignan, C. C.; Blum, A.; Balan, S. A.; Higgins, C. P.; Sunderland, E. M. Detection of Polyand Perfluoroalkyl Substances (PFASs) in U.S. Drinking Water Linked to Industrial Sites, Military Fire Training Areas, and Wastewater Treatment Plants. *Environ. Sci. Technol. Lett.* **2016**, 3, 344–350.
- (5) Anderson, R. H.; Thompson, T.; Stroo, H. F.; Leeson, A. US Department of Defense—Funded Fate and Transport Research on Per- and Polyfluoroalkyl Substances at Aqueous Film—Forming Foam—Impacted Sites. *Environ. Toxicol. Chem.* **2021**, *40*, 37–43.
- (6) Lifetime Drinking Water Health Advisories for Four Perfluoroalkyl Substances; U.S. Environmental Protection Agency: Washington, DC, 2022.
- (7) Moody, C. A.; Field, J. A. Determination of Perfluorocarboxylates in Groundwater Impacted by Fire-Fighting Activity. *Environ. Sci. Technol.* **1999**, *33*, 2800–2806.
- (8) Schultz, M. M.; Barofsky, D. F.; Field, J. A. Quantitative Determination of Fluorotelomer Sulfonates in Groundwater by LC MS/MS. *Environ. Sci. Technol.* **2004**, *38*, 1828–1835.
- (9) Backe, W. J.; Day, T. C.; Field, J. A. Zwitterionic, Cationic, and Anionic Fluorinated Chemicals in Aqueous Film Forming Foam Formulations and Groundwater from U.S. Military Bases by Nonaqueous Large-Volume Injection HPLC-MS/MS. *Environ. Sci. Technol.* **2013**, *47*, 5226–5234.
- (10) Houtz, E. F.; Sedlak, D. L. Oxidative Conversion as a Means of Detecting Precursors to Perfluoroalkyl Acids in Urban Runoff. *Environ. Sci. Technol.* **2012**, *46*, 9342–9349.
- (11) Song, Z.; Tang, H.; Wang, N.; Zhu, L. Reductive Defluorination of Perfluorooctanoic Acid by Hydrated Electrons in a Sulfite-Mediated UV Photochemical System. *J. Hazard. Mater.* **2013**, 262, 332–338.
- (12) Gu, Y.; Dong, W.; Luo, C.; Liu, T. Efficient Reductive Decomposition of Perfluorooctane Sulfonate in a High Photon Flux UV/Sulfite System. *Environ. Sci. Technol.* **2016**, *50*, 10554–10561.
- (13) Gu, Y.; Liu, T.; Zhang, Q.; Dong, W. Efficient Decomposition of Perfluorooctanoic Acid by a High Photon Flux UV/Sulfite Process: Kinetics and Associated Toxicity. *Chem. Eng. J.* **2017**, 326, 1125–1133
- (14) Tenorio, R.; Liu, J.; Xiao, X.; Maizel, A.; Higgins, C. P.; Schaefer, C. E.; Strathmann, T. J. Destruction of Per- and Polyfluoroalkyl Substances (PFASs) in Aqueous Film-Forming Foam (AFFF) with UV-Sulfite Photoreductive Treatment. *Environ. Sci. Technol.* **2020**, *54*, 6957–6967.
- (15) Bentel, M. J.; Yu, Y.; Xu, L.; Li, Z.; Wong, B. M.; Men, Y.; Liu, J. Defluorination of Per- and Polyfluoroalkyl Substances (PFASs) with Hydrated Electrons: Structural Dependence and Implications to PFAS Remediation and Management. *Environ. Sci. Technol.* **2019**, *53*, 3718–3728.
- (16) Bentel, M. J.; Yu, Y.; Xu, L.; Kwon, H.; Li, Z.; Wong, B. M.; Men, Y.; Liu, J. Degradation of Perfluoroalkyl Ether Carboxylic Acids with Hydrated Electrons: Structure—Reactivity Relationships and Environmental Implications. *Environ. Sci. Technol.* **2020**, *54*, 2489—2499.
- (17) Liu, C. J.; McKay, G.; Jiang, D.; Tenorio, R.; Cath, J. T.; Amador, C.; Murray, C. C.; Brown, J. B.; Wright, H. B.; Schaefer, C.;

- Higgins, C. P.; Bellona, C.; Strathmann, T. J. Pilot-Scale Field Demonstration of a Hybrid Nanofiltration and UV-Sulfite Treatment Train for Groundwater Contaminated by per- and Polyfluoroalkyl Substances (PFASs). *Water Res.* **2021**, 205, 117677.
- (18) Cui, J.; Gao, P.; Deng, Y. Destruction of Per- and Polyfluoroalkyl Substances (PFAS) with Advanced Reduction Processes (ARPs): A Critical Review. *Environ. Sci. Technol.* **2020**, 54, 3752–3766.
- (19) Bentel, M. J.; Liu, Z.; Yu, Y.; Gao, J.; Men, Y.; Liu, J. Enhanced Degradation of Perfluorocarboxylic Acids (PFCAs) by UV/Sulfite Treatment: Reaction Mechanisms and System Efficiencies at PH 12. *Environ. Sci. Technol. Lett.* **2020**, *7*, 351–357.
- (20) Buxton, G. V.; Greenstock, C. L.; Helman, W. P.; Ross, A. B. Critical Review of Rate Constants for Reactions of Hydrated Electrons, Hydrogen Atoms and Hydroxyl Radicals (·OH/·O– in Aqueous Solution. *J. Phys. Chem. Ref. Data* 1988, 17, 513–886.
- (21) Deister, U.; Warneck, P. Photooxidation of Sulfite (SO32-) in Aqueous Solution. *J. Phys. Chem.* **1990**, *94*, 2191–2198.
- (22) Park, H.; Vecitis, C. D.; Cheng, J.; Choi, W.; Mader, B. T.; Hoffmann, M. R. Reductive Defluorination of Aqueous Perfluorinated Alkyl Surfactants: Effects of Ionic Headgroup and Chain Length. *J. Phys. Chem. A* **2009**, *113*, 690–696.
- (23) Liu, Z.; Bentel, M. J.; Yu, Y.; Ren, C.; Gao, J.; Pulikkal, V. F.; Sun, M.; Men, Y.; Liu, J. Near-Quantitative Defluorination of Perfluorinated and Fluorotelomer Carboxylates and Sulfonates with Integrated Oxidation and Reduction. *Environ. Sci. Technol.* **2021**, *55*, 7052–7062.
- (24) Gao, J.; Liu, Z.; Bentel, M. J.; Yu, Y.; Men, Y.; Liu, J. Defluorination of Omega-Hydroperfluorocarboxylates (ω-HPFCAs): Distinct Reactivities from Perfluoro and Fluorotelomeric Carboxylates. *Environ. Sci. Technol.* **2021**, *55*, 14146–14155.
- (25) Barzen-Hanson, K. A.; Roberts, S. C.; Choyke, S. J.; Oetjen, K.; McAlees, A.; Riddell, N.; McCrindle, R.; Ferguson, P. L.; Higgins, C. P.; Field, J. A. Discovery of 40 Classes of Per- and Polyfluoroalkyl Substances in Historical Aqueous Film-Forming Foams (AFFFs) and AFFF-Impacted Groundwater. *Environ. Sci. Technol.* **2017**, *51*, 2047–2057
- (26) D'Agostino, L. A.; Mabury, S. A. Identification of Novel Fluorinated Surfactants in Aqueous Film Forming Foams and Commercial Surfactant Concentrates. *Environ. Sci. Technol.* **2014**, 48, 121–129.
- (27) Murray, C. C.; Vatankhah, H.; McDonough, C. A.; Nickerson, A.; Hedtke, T. T.; Cath, T. Y.; Higgins, C. P.; Bellona, C. L. Removal of Per- and Polyfluoroalkyl Substances Using Super-Fine Powder Activated Carbon and Ceramic Membrane Filtration. *J. Hazard. Mater.* **2019**, *366*, 160–168.
- (28) Schaefer, C. E.; Choyke, S.; Ferguson, P. L.; Andaya, C.; Burant, A.; Maizel, A.; Strathmann, T. J.; Higgins, C. P. Electrochemical Transformations of Perfluoroalkyl Acid (PFAA) Precursors and PFAAs in Groundwater Impacted with Aqueous Film Forming Foams. *Environ. Sci. Technol.* **2018**, *52*, 10689–10697.
- (29) Liu, C. J.; Strathmann, T. J.; Bellona, C. Rejection of Per- and Polyfluoroalkyl Substances (PFASs) in Aqueous Film-Forming Foam by High-Pressure Membranes. *Water Res.* **2021**, *188*, 116546.
- (30) Hao, S.; Choi, Y.-J.; Wu, B.; Higgins, C. P.; Deeb, R.; Strathmann, T. J. Hydrothermal Alkaline Treatment for Destruction of Per- and Polyfluoroalkyl Substances in Aqueous Film-Forming Foam. *Environ. Sci. Technol.* **2021**, *55*, 3283–3295.
- (31) Nickerson, A.; Maizel, A. C.; Kulkarni, P. R.; Adamson, D. T.; Kornuc, J. J.; Higgins, C. P. Enhanced Extraction of AFFF-Associated PFASs from Source Zone Soils. *Environ. Sci. Technol.* **2020**, *54*, 4952–4962.
- (32) Shoemaker, J. A.; Grimmett, P.; Boutin, B. Determination of Selected Perfluorinated Alkyl Acids in Drinking Water by Solid Phase Extraction and Liquid Chromatography/Tandem Mass Spectrometry (LC/MS/MS). U.S. Environmental Protection Agency: Washington, DC, 2008.
- (33) Krauss, M.; Singer, H.; Hollender, J. LC-High Resolution MS in Environmental Analysis: From Target Screening to the

- Identification of Unknowns. Anal. Bioanal. Chem. 2010, 397, 943-951.
- (34) Kern, S.; Fenner, K.; Singer, H. P.; Schwarzenbach, R. P.; Hollender, J. Identification of Transformation Products of Organic Contaminants in Natural Waters by Computer-Aided Prediction and High-Resolution Mass Spectrometry. *Environ. Sci. Technol.* **2009**, *43*, 7039–7046.
- (35) Martin, J. W.; Kannan, K.; Berger, U.; Voogt, P. D.; Field, J.; Franklin, J.; Giesy, J. P.; Harner, T.; Muir, D. C. G.; Scott, B.; Kaiser, M.; Järnberg, U.; Jones, K. C.; Mabury, S. A.; Schroeder, H.; Simcik, M.; Sottani, C.; Bavel, B. V.; Kärrman, A.; Lindström, G.; et al. Peer Reviewed: Analytical Challenges Hamper Perfluoroalkyl Research. *Environ. Sci. Technol.* **2004**, *38*, 248A–255A.
- (36) Narizzano, A. M.; Bohannon, M. E.; East, A. G.; McDonough, C.; Choyke, S.; Higgins, C. P.; Quinn, M. J., Jr Patterns in Serum Toxicokinetics in Peromyscus Exposed to Per- and Polyfluoroalkyl Substances. *Environ. Toxicol. Chem.* **2021**, *40*, 2886–2898.
- (37) Schymanski, E. L.; Jeon, J.; Gulde, R.; Fenner, K.; Ruff, M.; Singer, H. P.; Hollender, J. Identifying Small Molecules via High Resolution Mass Spectrometry: Communicating Confidence. *Environ. Sci. Technol.* **2014**, *48*, 2097–2098.
- (38) Dinglasan, M. J. A.; Ye, Y.; Edwards, E. A.; Mabury, S. A. Fluorotelomer Alcohol Biodegradation Yields Poly- and Perfluorinated Acids. *Environ. Sci. Technol.* **2004**, *38*, 2857–2864.
- (39) Liu, Y.; Pereira, A. D. S.; Martin, J. W. Discovery of C5–C17 Poly- and Perfluoroalkyl Substances in Water by In-Line SPE-HPLC-Orbitrap with In-Source Fragmentation Flagging. *Anal. Chem.* **2015**, 87, 4260–4268.
- (40) Tseng, N.; Wang, N.; Szostek, B.; Mahendra, S. Biotransformation of 6:2 Fluorotelomer Alcohol (6:2 FTOH) by a Wood-Rotting Fungus. *Environ. Sci. Technol.* **2014**, *48*, 4012–4020.
- (41) Moe, M. K.; Huber, S.; Svenson, J.; Hagenaars, A.; Pabon, M.; Trümper, M.; Berger, U.; Knapen, D.; Herzke, D. The Structure of the Fire Fighting Foam Surfactant Forafac[®]1157 and Its Biological and Photolytic Transformation Products. *Chemosphere* **2012**, *89*, 869–875.
- (42) Weiner, B.; Yeung, L. W. Y.; Marchington, E. B.; D'Agostino, L. A.; Mabury, S. A. Organic Fluorine Content in Aqueous Film Forming Foams (AFFFs) and Biodegradation of the Foam Component 6: 2 Fluorotelomermercaptoalkylamido Sulfonate (6: 2 FTSAS). *Environ. Chem.* **2013**, *10*, 486–493.
- (43) Field, J. A.; Schultz, M.; Barofsky, D. Identifying Hydrocarbon and Fluorocarbon Surfactants in Specialty Chemical Formulations of Environmental Interest by Fast Atom Bombardment/Mass Spectrometry. *Chim. Int. J. Chem.* **2003**, *57*, 556–560.
- (44) Baduel, C.; Mueller, J. F.; Rotander, A.; Corfield, J.; Gomez-Ramos, M.-J. Discovery of Novel Per- and Polyfluoroalkyl Substances (PFASs) at a Fire Fighting Training Ground and Preliminary Investigation of Their Fate and Mobility. *Chemosphere* **2017**, *185*, 1030–1038.
- (45) Ahrens, L.; Siebert, U.; Ebinghaus, R. Total Body Burden and Tissue Distribution of Polyfluorinated Compounds in Harbor Seals (Phoca Vitulina) from the German Bight. *Mar. Pollut. Bull.* **2009**, *58*, 520–525.
- (46) Allred, B. M.; Lang, J. R.; Barlaz, M. A.; Field, J. A. Physical and Biological Release of Poly- and Perfluoroalkyl Substances (PFASs) from Municipal Solid Waste in Anaerobic Model Landfill Reactors. *Environ. Sci. Technol.* **2015**, *49*, 7648–7656.
- (47) Nguyen, V. T.; Reinhard, M.; Karina, G. Y.-H. Occurrence and Source Characterization of Perfluorochemicals in an Urban Watershed. *Chemosphere* **2011**, *82*, 1277–1285.
- (48) De Silva, A. O.; Spencer, C.; Scott, B. F.; Backus, S.; Muir, D. C. G. Detection of a Cyclic Perfluorinated Acid, Perfluoroethylcyclohexane Sulfonate, in the Great Lakes of North America. *Environ. Sci. Technol.* **2011**, *45*, 8060–8066.
- (49) Braams, R. Rate Constants of Hydrated Electron Reactions with Amino Acids. *Radiat. Res.* **1966**, 27, 319–329.
- (50) Garrison, W. M. Reaction Mechanisms in the Radiolysis of Peptides, Polypeptides, and Proteins. *Chem. Rev.* **1987**, *87*, 381–398.

- (51) Liu, J.; Van Hoomissen, D. J.; Liu, T.; Maizel, A.; Huo, X.; Fernández, S. R.; Ren, C.; Xiao, X.; Fang, Y.; Schaefer, C.; Higgins, C. P.; Vyas, S.; Strathmann, T. J. Reductive Defluorination of Branched Per- and Polyfluoroalkyl Substances with Cobalt Complex Catalysts. Environ. Sci. Technol. Lett. 2018, 5, 289-294.
- (52) Hart, E. J.; Gordon, S.; Thomas, J. K. Rate Constants of Hydrated Electron Reactions with Organic Compounds1. J. Phys. Chem. 1964, 68, 1271-1274.
- (53) Rustgi, S.; Joshi, A.; Riesz, P.; Friedberg, F. E.S.R. of Spin-Trapped Radicals in Aqueous Solutions of Amino Acids. Int. J. Radiat. Biol. Relat. Stud. Phys. Chem. Med. 1977, 32, 533-552.
- (54) Anbar, M. The Reactions of Hydrated Electrons with Organic Compounds. Adv. Phys. Org. Chem. 1969, 7, 115–151.
- (55) Kerzig, C.; Guo, X.; Wenger, O. S. Unexpected Hydrated Electron Source for Preparative Visible-Light Driven Photoredox Catalysis. J. Am. Chem. Soc. 2019, 141, 2122-2127.
- (56) Harding-Marjanovic, K. C.; Houtz, E. F.; Yi, S.; Field, J. A.; Sedlak, D. L.; Alvarez-Cohen, L. Aerobic Biotransformation of Fluorotelomer Thioether Amido Sulfonate (Lodyne) in AFFF-Amended Microcosms. Environ. Sci. Technol. 2015, 49, 7666-7674.
- (57) Liu, M.; Munoz, G.; Vo Duy, S.; Sauvé, S.; Liu, J. Stability of Nitrogen-Containing Polyfluoroalkyl Substances in Aerobic Soils. Environ. Sci. Technol. 2021, 55, 4698-4708.
- (58) Houtz, E. F.; Higgins, C. P.; Field, J. A.; Sedlak, D. L. Persistence of Perfluoroalkyl Acid Precursors in AFFF-Impacted Groundwater and Soil. Environ. Sci. Technol. 2013, 47, 8187-8195.
- (59) Rhoads, K. R.; Janssen, E. M.-L.; Luthy, R. G.; Criddle, C. S. Aerobic Biotransformation and Fate of N-Ethyl Perfluorooctane Sulfonamidoethanol (N-EtFOSE) in Activated Sludge. Environ. Sci. Technol. 2008, 42, 2873-2878.
- (60) Bruton, T. A.; Sedlak, D. L. Treatment of Aqueous Film-Forming Foam by Heat-Activated Persulfate Under Conditions Representative of In Situ Chemical Oxidation. Environ. Sci. Technol. 2017, 51, 13878-13885.
- (61) Strynar, M.; Dagnino, S.; McMahen, R.; Liang, S.; Lindstrom, A.; Andersen, E.; McMillan, L.; Thurman, M.; Ferrer, I.; Ball, C. Identification of Novel Perfluoroalkyl Ether Carboxylic Acids (PFECAs) and Sulfonic Acids (PFESAs) in Natural Waters Using Accurate Mass Time-of-Flight Mass Spectrometry (TOFMS). Environ. Sci. Technol. 2015, 49, 11622-11630.

□ Recommended by ACS

An Integrated Approach for Determination of Total Per- and Polyfluoroalkyl Substances (PFAS)

Marzieh Shojaei, Jennifer L. Guelfo, et al.

OCTORER 05 2022

ENVIRONMENTAL SCIENCE & TECHNOLOGY

READ 2

PhotoTOP: PFAS Precursor Characterization by UV/TiO, **Photocatalysis**

Jonathan Zweigle, Christian Zwiener, et al.

OCTOBER 28, 2022

ENVIRONMENTAL SCIENCE & TECHNOLOGY

READ **C**

An Investigation of Thermal Air Degradation and Pyrolysis of Per- and Polyfluoroalkyl Substances and Aqueous Film-**Forming Foams in Soil**

Ali Alinezhad, Feng Xiao, et al.

JANUARY 11, 2022

ACS ES&T ENGINEERING

RFAD 17

Release of Volatile Per- and Polyfluoroalkyl Substances from **Aqueous Film-Forming Foam**

Julia Roth, David Hanigan, et al.

FEBRUARY 20, 2020

ENVIRONMENTAL SCIENCE & TECHNOLOGY LETTERS

READ **C**

Get More Suggestions >

Supporting Information

Application of high-resolution mass spectrometry to evaluate UV-sulfiteinduced transformations of per- and polyfluoroalkyl substances (PFASs) in aqueous film-forming foam (AFFF)

Raul Tenorio, †,‡,§ Andrew C. Maizel,‡, Charles E. Schaefer, Christopher P. Higgins,‡ and Timothy J. Strathmann.‡*

- †. University of Illinois at Urbana-Champaign, Department of Civil and Environmental Engineering, 205 North Mathews Avenue, Urbana, Illinois 61801, USA.
- ‡. Colorado School of Mines, Department of Civil and Environmental Engineering, 1500 Illinois Street, Golden, Colorado 80401, USA.
 - §. Haley & Aldrich, 400 E Van Buren St #545, Phoenix, AZ 85004, USA. (Current Affiliation)
 - ||. Institute for Soft Matter Synthesis and Metrology, Georgetown University, Washington, District of Columbia, 20057, USA.
 - L. CDM Smith, 110 Fieldcrest Avenue, Edison, New Jersey 08837, USA.

*Corresponding author: E-mail: strthmnn@mines.edu

12 pages

3 tables

5 figures

S1. Chemical Reagents

Sodium sulfite (Sigma-Aldrich, \geq 98%), sodium bicarbonate (Macron, ACS grade), sodium hydroxide (Fisher, 1 N), hydrochloric acid (Fluka, 1 N), sodium phosphate monobasic dihydrate (Sigma-Aldrich, \geq 99%), ammonium hydroxide (Fisher, Optima grade), ammonium acetate (Fisher, Optima grade), methanol (Fisher, Optima LC/MS grade), and isopropanol (Fisher, Optima LC/MS grade) were used in this study. All solutions were prepared using deionized water (Millipore system, ASTM Type I). The AFFF concentrate mixture that was diluted 1-to-60,000 fold for UV-sulfite reactions is described in the Materials and Methods Section.

S2. Figures and Tables

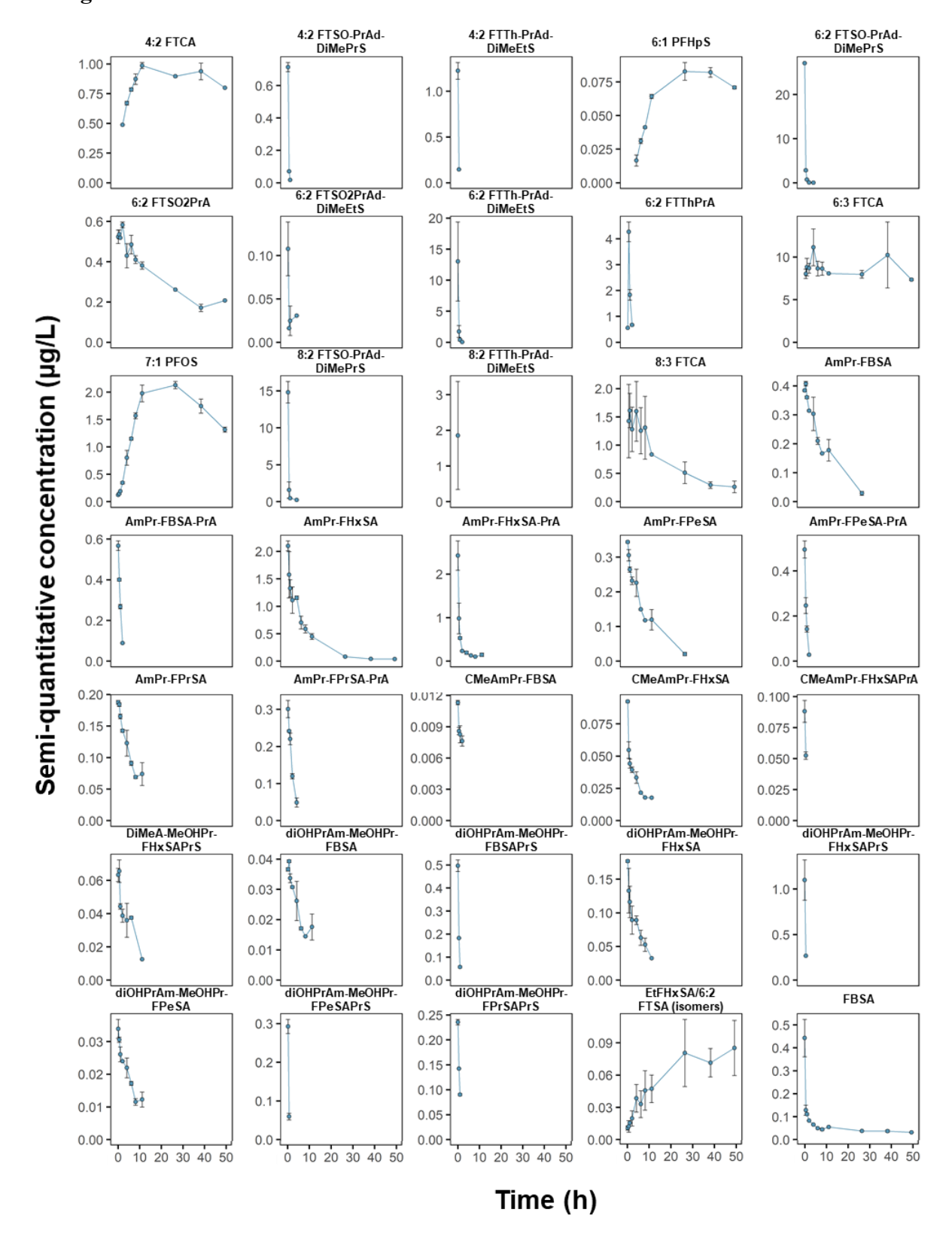


Figure S1. Timecourses for individual PFASs detected by LC-QTOF-MS suspect screening analysis.

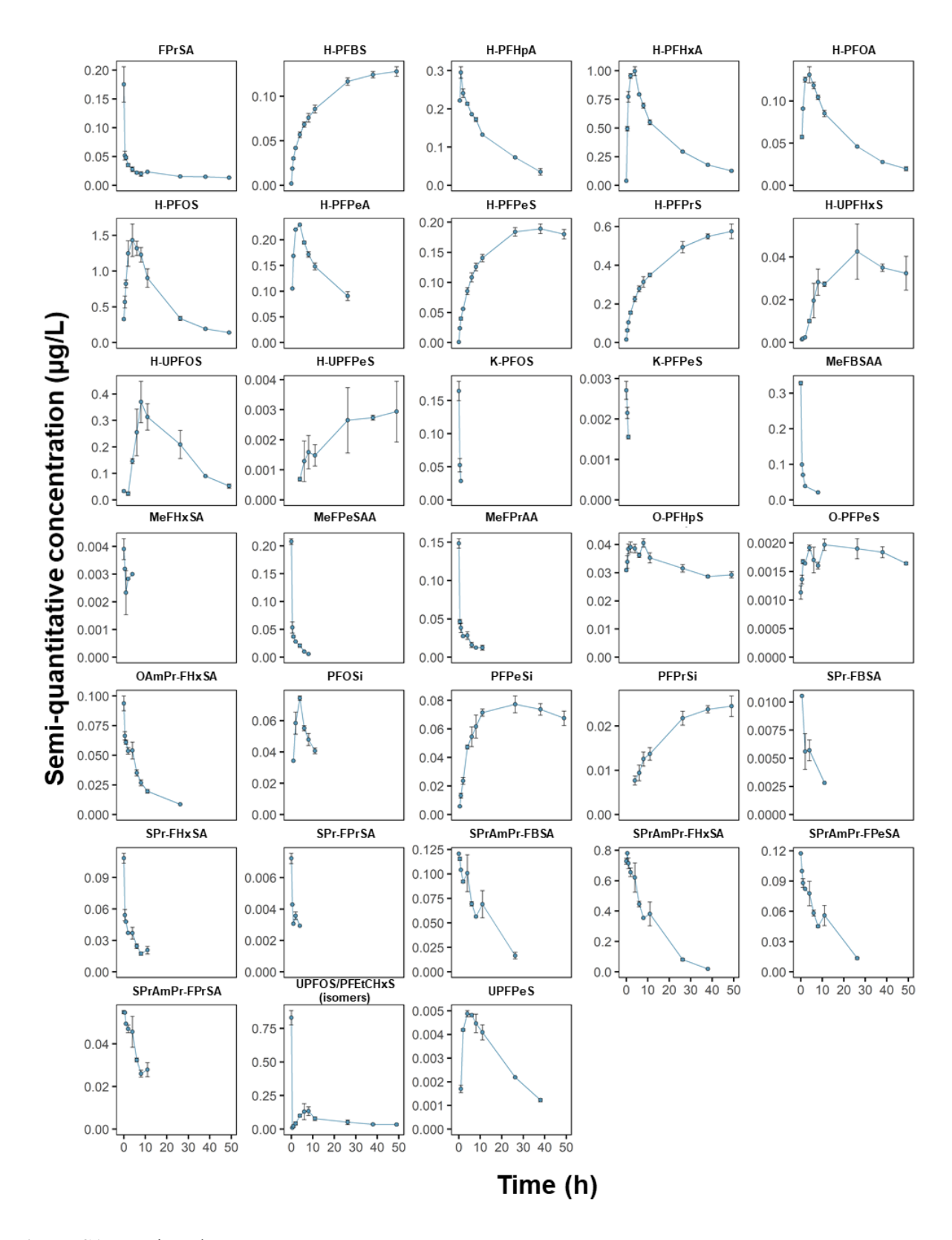


Figure S1. Continued.

Table S1. PFASs with at least 1 spectral library match >70% in reaction timecourses.

PFAS	Library hits in timecourse ^a
4:2 FTSO-PrAd-DiMePrS	2
6:2 FTSO-PrAd-DiMePrS	6
6:2 FTTh-PrAd-DiMeEtS	3
7:1 PFOS	14
8:2 FTSO-PrAd-DiMePrS	3
8:2 FTTh-PrAd-DiMeEtS	1
AmPr-FHxSA	4
AmPr-FHxSA-PrA	4
AmPr-FPeSA	6
AmPr-FPrSA-PrA	7
DiMeA-MeOHPr-FHxSAPrS	1
diOHPrAm-MeOHPr-FBSA	2
diOHPrAm-MeOHPr-FPeSA	6
FBSA	14
FPrSA	6
H-PFOA	1
H-UPFOS	2
K-PFOS	1
SPrAmPr-FBSA	9
SPrAmPr-FHxSA	18
SPrAmPr-FPeSA	16
SPrAmPr-FPrSA	5
SPr-FHxSA	1

^aTotal number of points in PFAS reaction timecourse with spectral library match >70% out of 22 total points (11 time points in duplicate).

Table S2. List of PFASs and PFAS class names for analytes detected by LC-QTOF-MS targeted and suspect screening analysis.

Super Class	Class Acronym	Class Name	Compound Acronym	Compound Name
Perfluoroalkyl	PFSA	perfluoroalkane sulfonate	PFNS	perfluorononane sulfonate
acids (PFAAs)			PFOS	perfluorooctane sulfonate
			PFHpS	perfluoroheptane sulfonate
			PFHxS	perfluorohexane sulfonate
			PFPeS	perfluoropentane sulfonate
			PFBS	perfluorobutane sulfonate
			PFPrS	perfluoropropane sulfonate
	PFCA	perfluoroalkanoic acid	PFOA	perfluorooctanoic acid
			PFHpA	perfluoroheptanoic acid
			PFHxA	perfluorohexanoic acid
			PFPeA	perfluoropentanoic acid
			PFBA	perfluorobutanoic acid
Fluorotelomer	X:2 FTS	X:2 fluorotelomer sulfonate	8:2 FTS	8:2 fluorotelomer sulfonate
sulfonic acids (FTSs) and			6:2 FTS	6:2 fluorotelomer sulfonate
fluorotelomer			4:2 FTS	4:2 fluorotelomer sulfonate
carboxylic acids	X:2 FTCA	X:2 fluorotelomer carboxylic acid	4:2 FTCA	4:2 fluorotelomer carboxylic acid
(FTCAs)	X:3 FTCA	X:3 fluorotelomer carboxylic acid	8:3 FTCA	8:3 fluorotelomer carboxylic acid
			6:3 FTCA	6:3 fluorotelomer carboxylic acid
Fluorotelomer	X:2 FTSA	X:2 fluorotelomer sulfonamide	6:2 FTSA	6:2 fluorotelomer sulfonamide
sulfonic acid (FTS) and fluorotelomer carboxylic acid	X:2 FTSO2PrAd- DiMeEtS X:2 FTSO-PrAd- DiMePrS	X:2 fluorotelomer sulfonyl propanoamido- dimethyl ethyl sulfonate	6:2 FTSO2PrAd- DiMeEtS	6:2 fluorotelomer sulfonyl propanoamido-dimethylethyl sulfonate
		X:2 fluorotelomer sulfinyl propanamido dimethyl ethyl sulfonate	8:2 FTSO-PrAd- DiMePrS	8:2 fluorotelomer sulfinyl propanamido dimethyl ethyl sulfonate
(FTCA) derivatives			6:2 FTSO-PrAd- DiMePrS	6:2 fluorotelomer sulfinyl propanamido dimethyl ethyl sulfonate
			4:2 FTSO-PrAd- DiMePrS	4:2 fluorotelomer sulfinyl propanamido dimethyl ethyl sulfonate
	X:2 FTThPrA	X:2 fluorotelomer thia propanoic acid	6:2 FTThPrA	6:2 fluorotelomer thia propanoic acid
	X:2 FTTh-PrAd- X:2 fluorotelomer thia propanoamido ethyl sulfonate		8:2 FTTh-PrAd-DiMeEtS	8:2 fluorotelomer thia propanoamido dimethyl ethyl sulfonate
			6:2 FTTh-PrAd-DiMeEtS	6:2 fluorotelomer thia propanoamido dimethyl ethyl sulfonate
			4:2 FTTh-PrAd-DiMeEtS	4:2 fluorotelomer thia propanoamido dimethyl ethyl sulfonate
Fluorotelomer sulfonates/sulfates	X:2 FTSO2PrA	X:2 fluorotelomersulfonyl propanoic acid	6:2 FTSO2PrA	6:2 fluorotelomersulfonyl propanoic acid
Suitonates/suitates Perfluoroalkyl	PFSAi	perfluoroalkanesulfinate	PFOSi	perfluorooctane sulfinate
sulfonic acid		•	PFPeSi	perfluoropentane sulfinate
(PFSA) derivatives			PFPrSi	perfluoropropane sulfinate
uenvalives				1 1 1

Table S2. Continued.

Super Class	Class Acronym	Class Name	Compound Acronym	Compound Name
Substituted	H-PFCA	hydrido-perfluoroalkanoic acid	H-PFOA	Hydrido-perfluorooctanoic acid
perfluoroalkyl			H-PFHpA	Hydrido-perfluoroheptanoic acid
acid (PFAA) derivatives			H-PFHxA	Hydrido-perfluorohexanoic acid
delivatives			H-PFPeA	Hydrido-perfluoropentanoic acid
	H-PFSA	hydrido-perfluoroalkane sulfonate	H-PFOS	Hydrido-PerFluoroOctane Sulfonate
			H-PFPeS	Hydrido-PerFluoroPentane Sulfonate
			H-PFBS	Hydrido-PerFluoroButane Sulfonate
			H-PFPrS	Hydrido-PerFluoroPropane Sulfonate
	K-PFSA	keto-perfluoroalkanesulfonate	K-PFOS	Keto-perfluorooctane sulfonate
			K-PFPeS	Keto-perfluoropentane sulfonate
	O-PFSA	oxa-perfluoroalkanesulfonate	O-PFHpS	Oxa-perfluoroheptane sulfonate
			O-PFPeS	Oxa-perfluoropentane sulfonate
	X:1 PFSA	X:1 perfluoroalkanesulfonate	7:1 PFOS	7:1 perfluorooctane sulfonate
			6:1 PFHpS	6:1 perfluoroheptane sulfonate
Cyclic and	H-UPFSA	hydrido-unsaturated perfluoroalkane	H-UPFOS	Hydrido-Unsaturated PerFluoroOctane Sulfonate
unsaturated		sulfonate	H-UPFHxS	Hydrido-Unsaturated PerFluoroHexane Sulfonate
perfluoroalkyl acids (PFAAs)			H-UPFPeS	Hydrido-Unsaturated PerFluoroPentane Sulfonate
acius (FFAAS)	UPFSA	unsaturated perfluoroalkane sulfonate	UPFOS	Unsaturated perfluorooctane sulfonate
			UPFPeS	Unsaturated perfluoropentane sulfonate
	CHxS	cyclohexane sulfonate	PFEtCHxS	perfluoro ethyl cyclohexane sulfonate
Sulfonamide	AmPr-FASA	N-dimethyl ammonio propyl perfluoroalkane sulfonamide	AmPr-FHxSA	N-dimethyl ammonio propyl perfluorohexane sulfonamide
Precursors			AmPr-FPeSA	N-dimethyl ammonio propyl perfluoropentane sulfonamide
			AmPr-FBSA	N-dimethyl ammonio propyl perfluorobutane sulfonamide
			AmPr-FPrSA	N-dimethyl ammonio propyl perfluoropropane sulfonamide
	AmPr-FASA-PrA	N-dimethyl ammonio propyl perfluoralkane sulfonamido propanoic acid	AmPr-FHxSA-PrA	N-dimethyl ammonio propyl perfluorohexane sulfonamido propanoic acid
			AmPr-FPeSA-PrA	N-dimethyl ammonio propyl perfluoropentane sulfonamido propanoic acid
			AmPr-FBSA-PrA	N-dimethyl ammonio propyl perfluorbutoane sulfonamido propanoic acid
			AmPr-FPrSA-PrA	N-dimethyl ammonio propyl perfluoropropane sulfonamido propanoic acid
	CMeAmPr-FASA	N-carboxymethyldimethylammoniopropyl-	CMeAmPr-FHxSA	N-Carboxymethyldimethylammoniopropyl-perfluorohexanesulfonamide
		perfluoroalkanesulfonamide	CMeAmPr-FBSA	N-Carboxymethyldimethylammoniopropyl-perfluorobutanesulfonamide
	CMeAmPr-FASAPrA	N-carboxymethyldimethylammoniopropylperfluoroalkanesulfonamido propanoic acid	CMeAmPr-FHxSAPrA	N-carboxymethyldimethyl ammoniopropyl-perfluorohexane sulfonamido propanoic acid
	DiMeA-MeOHPr- FASAPrS	N-dimethylaminohydroxymethyl propylperfluoroalkanesulfonamidopropylsulfonate	DiMeA-MeOHPr- FHxSAPrS	N-dimethylaminohydroxybutyl-perfluorohexanesulfonamidopropylsulfonate
	diOHPrAm-MeOHPr- FASA	n-MeOHPr- N-dihydrox propyldimethylammonio hydroxymethyl propyl perfluoroalkane sulfonamide	diOHPrAm-MeOHPr- FHxSA	N-dihydroxy propyl dimethyl ammonio hydroxymethyl propyl- perfluorohexanesulfonamide
			diOHPrAm-MeOHPr- FPeSA	N-dihydroxy propyl dimethyl ammonio hydroxymethyl propyl- perfluoropentanesulfonamide
			diOHPrAm-MeOHPr- FBSA	N-dihydroxy propyl dimethyl ammonio hydroxymethyl propyl- perfluorobutanesulfonamide

Table S2. Continued.

Super Class	Class Acronym	Class Name	Compound Acronym	Compound Name
	diOHPrAm-MeOHPr- FASAPrS	N-dihydroxy propyldimethylammoniohydroxymethylpropyl-	diOHPrAm-MeOHPr- FHxSAPrS	N-dihydroxy propyldimethyl ammoniohydroxymethyl propyl-perfluorohexane sulfonamido propyl sulfonate
		perfluoroalkane sulfonamidopropyl sulfonate	diOHPrAm-MeOHPr- FPeSAPrS	N-dihydroxy propyldimethyl ammoniohydroxymethyl propyl-perfluoropentane sulfonamidopropyl sulfonate
			diOHPrAm-MeOHPr- FBSAPrS	N-dihydroxy propyldimethyl ammoniohydroxymethyl propyl-perfuorobutane sulfonamido propyl sulfonate
			diOHPrAm-MeOHPr- FPrSAPrS	N-dihydroxy propyldimethyl ammoniohydroxymethyl propyl-perfluoropropane sulfonamido propyl sulfonate
	EtFASA	N-ethylperfluoro-1-alkanesulfonamide	EtFHxSA	N-ethylperfluoro-1-hexane sulfonamide
	FASA	perfluoroalkane sulfonamide	FBSA	perfluorobutane sulfonamide
			FPrSA	perfluoropropane sulfonamide
	MeFASA	N-methyl perfluoroalkane sulfonamide	MeFHxSA	N-methyl perfluoro-1-hexane sulfonamide
	MeFASAA	N-methylperfluoroalkanesulfonamidoacetic acid	MeFPeSAA	N-methylperfluoropentane sulfonamido acetic acid
			MeFBSAA	N-methylperfluorobutane sulfonamido acetic acid
			MeFPrSAA	N-methylperfluoropropane sulfonamido acetic acid
	FASA-PrA	perfluoroalkane sulfonamido propanoic acid	FPeSA-PrA	perfluoropentane sulfonamido propanoic acid
			FBSA-PrA	perfluorobutane sulfonamido propanoic acid
			FPrSA-PrA	Perfluoropropane sulfonamido propanoic acid
	OAmPr-FASA	N-oxidedimethylammoniopropyl- perfluoroalkanesulfonamide	OAmPr-FHxSA	N-oxidedimethylammoniopropyl-perfluorohexanesulfonamide
	SPrAmPr-FASA	N-sulfo propyl dimethyl ammonio propyl perfluoroalkanesulfonamide	SPrAmPr-FHxSA	N-sulfo propyl dimethyl ammonio propyl perfluorohexane sulfonamide
			SPrAmPr-FPeSA	N-sulfo propyl dimethyl ammonio propyl perfluoropentane sulfonamide
			SPrAmPr-FBSA	N-sulfo propyl dimethyl ammonio propyl perfluorobutane sulfonamide
			SPrAmPr-FPrSA	N-sulfo propyl dimethyl ammonio propyl perfluoropropane sulfonamide
	SPr-FASA	N-sulfo propyl perfluoroalkanesulfonamide	SPr-FHxSA	N-sulfo propyl perfluorohexane sulfonamide
			SPr-FBSA	N-sulfo propyl perfluorobutane sulfonamide
			SPr-FPrSA	N-sulfo propyl perfluoropropane sulfonamide

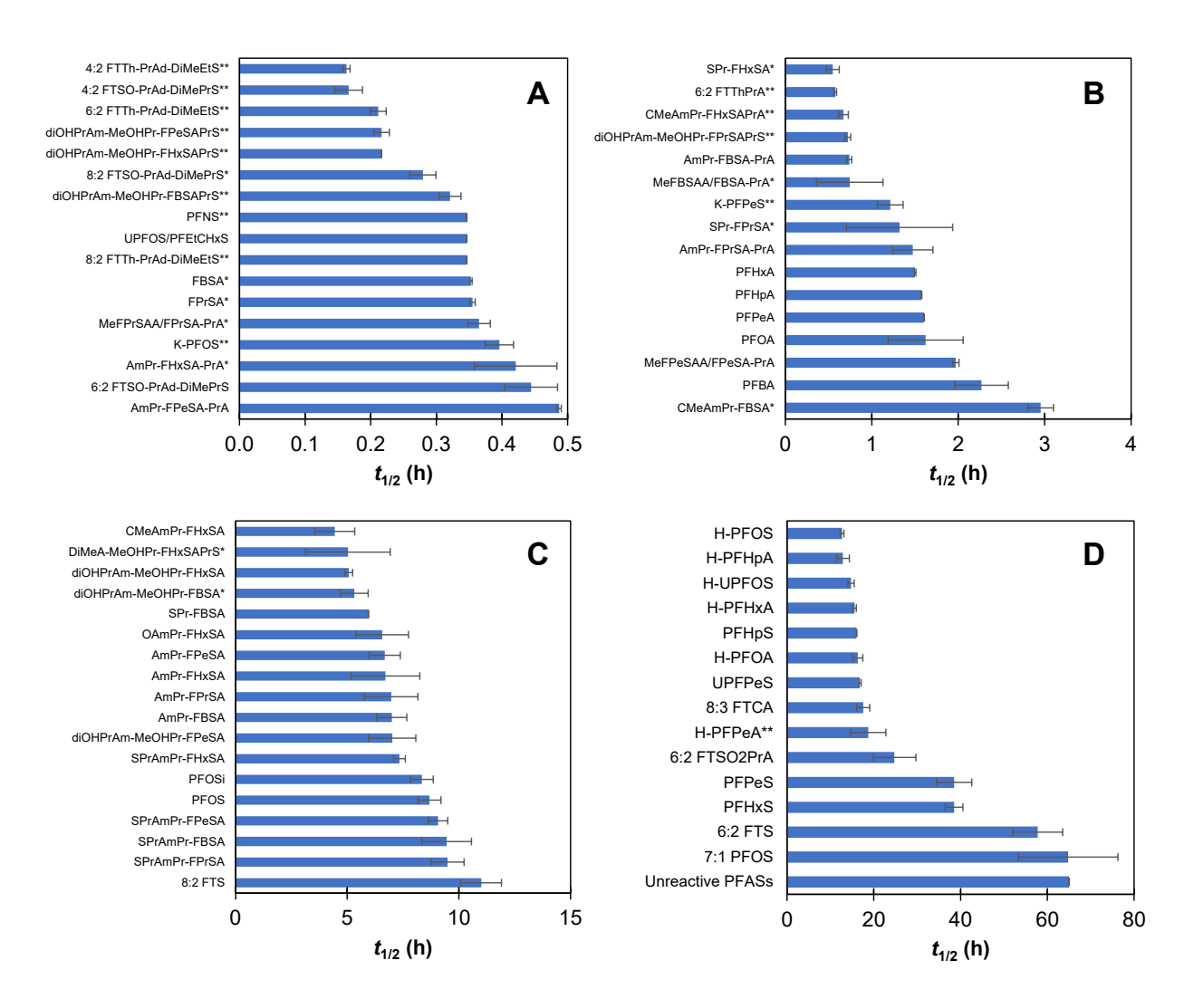


Figure S2. Half-lives $(t_{1/2})$ of individual PFASs observed during UV-sulfite treatment. Panels are organized by apparent reactivity: (A) compounds with $t_{1/2} = 0-0.5$ h, (B) $t_{1/2} = 0.5-4$ h, (C) $t_{1/2} = 4-12$, (D) $t_{1/2} = 12-65$ h. Half-life estimates for PFASs that did not follow first-order decay behavior are indicated by an asterisk (*). Half-lives calculated using 2-3-point k_{obs} estimates (and 1-point k_{obs} estimate for 8:2 FTTh-PrAd-DiMeEtS) are indicated by a double asterisk (**). The " \square " symbol in (D) indicates 18 PFASs that were observed to be unreactive during experiments (i.e., $t_{1/2} > 65$ h; Section "E" in Figure 2).

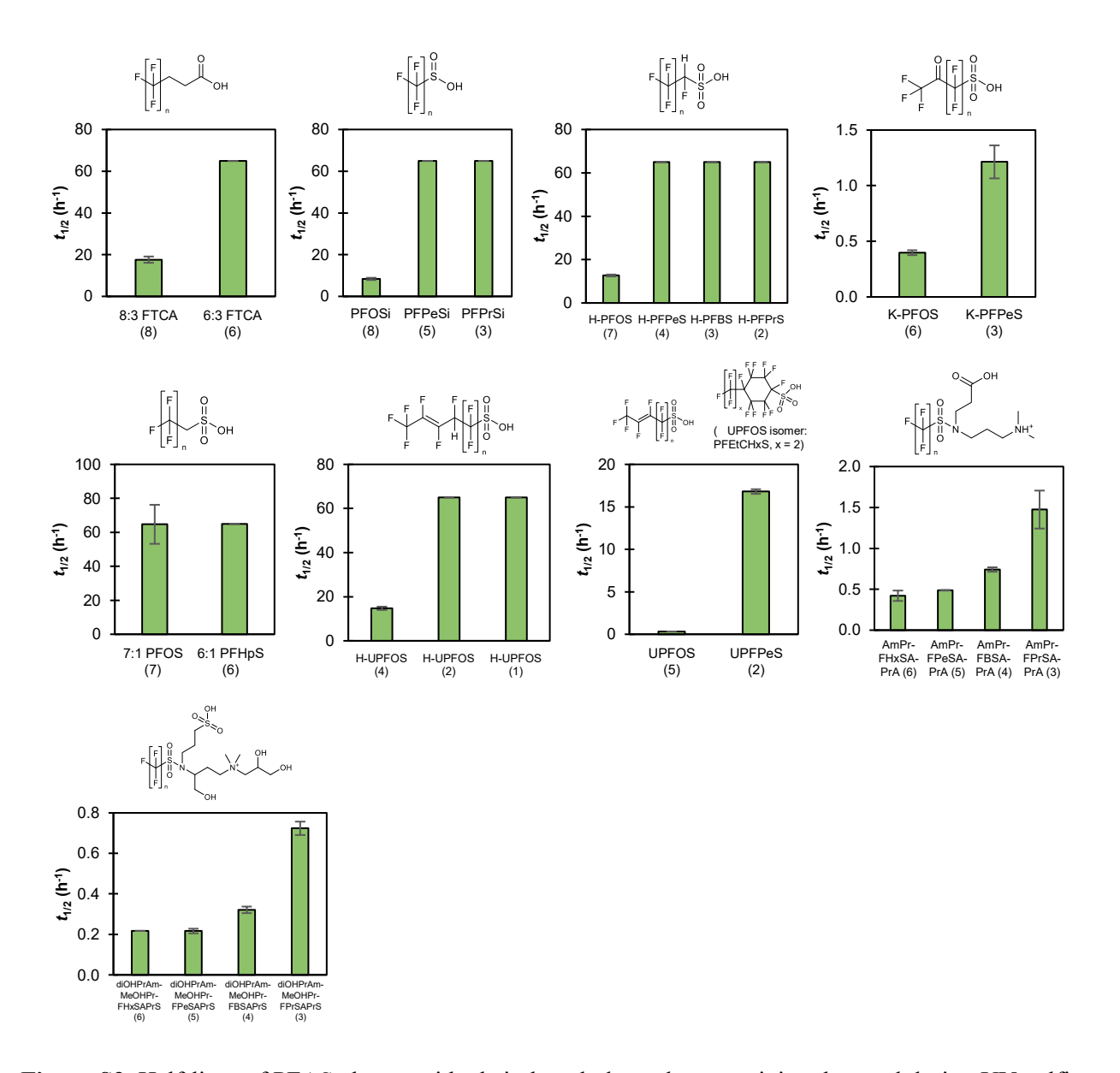


Figure S3. Half-lives of PFAS classes with chain length dependent reactivity observed during UV-sulfite treatment (generic structure for the class shown above each panel). Error bars extend to minimum and maximum values of replicate experiments. No error bars indicate a $t_{1/2}$ valued determined from a single replicate. PFEtCHxS, structural isomer of UPFOS, is indicated by the " \blacksquare " symbol. The " \blacklozenge " symbols indicate PFASs that were observed to be unreactive in experiments (i.e., $t_{1/2} > 65$ h).

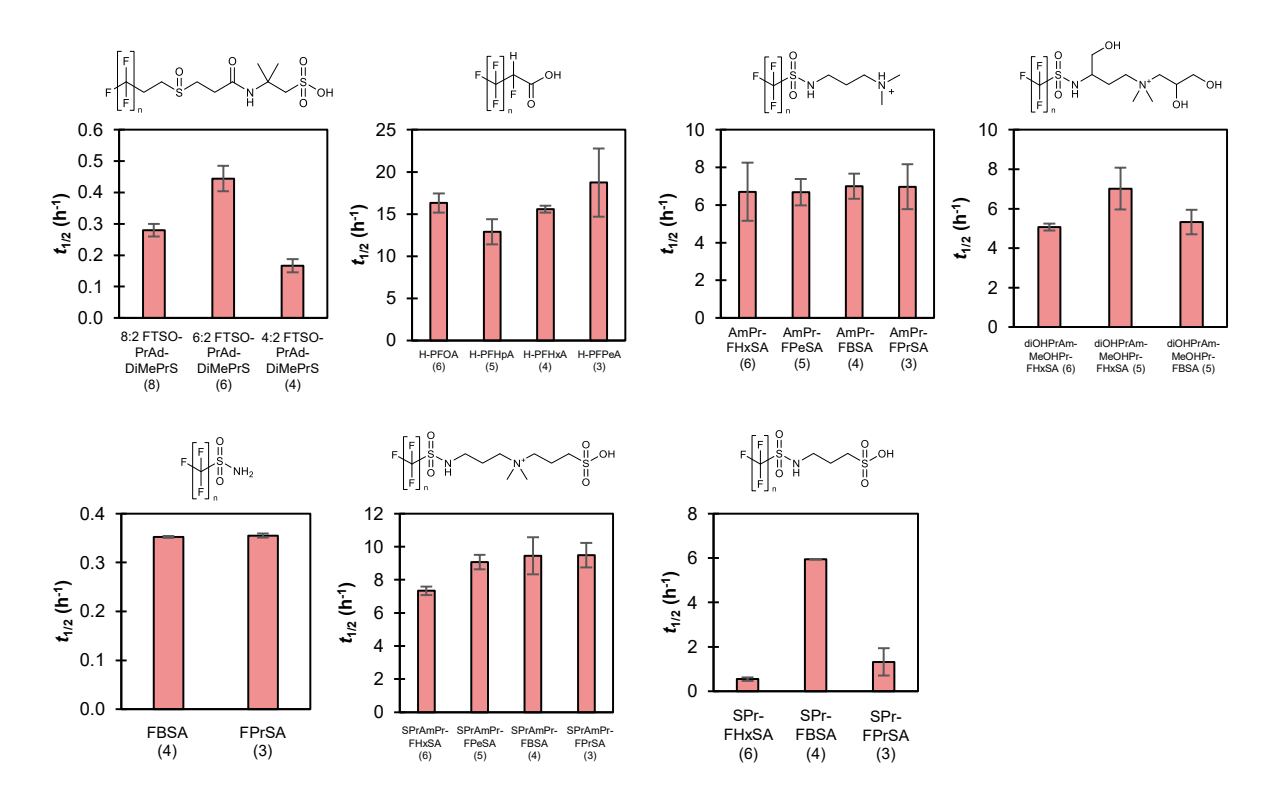


Figure S4. Half-lives of PFAS classes with chain length independent reactivity (generic structure for the class shown above each panel). Error bars extend to minimum and maximum values of replicate experiments. No error bars indicate a $t_{1/2}$ valued determined from a single replicate.

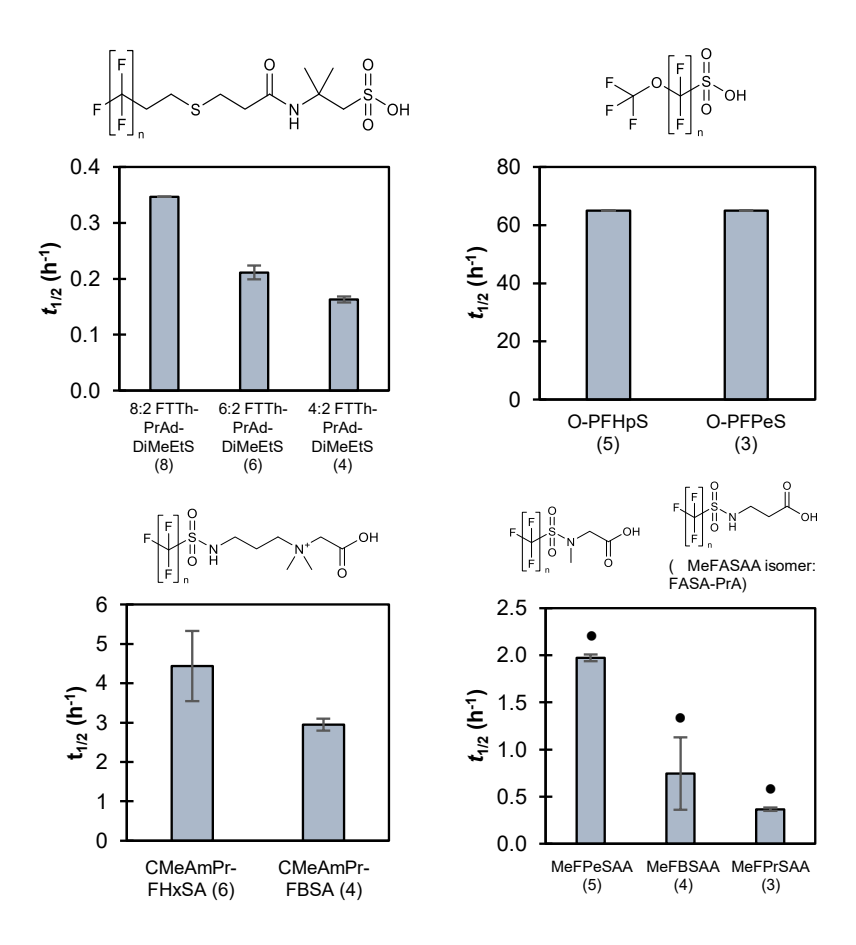


Figure S5. Half-lives of PFAS classes with special case chain length reactivity trends observed during UV-sulfite treatment (generic structure for the class shown above each panel). Error bars extend to minimum and maximum values of replicate experiments. No error bars indicate a $t_{1/2}$ value determined from a single replicate. The " \bullet " symbols indicate PFASs that were observed to be unreactive in experiments (i.e., $t_{1/2} > 65$ h).

Table S3. List of structural isomers.

Structure		Isomer		Neutral Formula
EtFHxSA (n = 6)	$F = \begin{bmatrix} F \\ S \\$	6:2 FTSA (n = 6)	F = F =	C8H6O2NSF13
UPFOS (n = 6)	F S OH	PFEtCHxS (n = 2)	F F F OH	C8HO3SF15
MeFASAA (n = 3, 4, 5)	$ \begin{array}{c c} F & 0 \\ S & 0 \\ S & 0 \\ F & 0 \\ S & 0 \end{array} $ OH	FASA-PrA (n = 3, 4, 5)	F O H OH	C6H6O4NSF7 (n = 3), C7H6O4NSF9 (n = 4), C8H6O4NSF11 (n = 5)